Living coccolithophores from the eastern equatorial Indian Ocean during the spring intermonsoon: Indicators of hydrography

*Jun Sun [1, 2,3], Haijiao Liu [1,2,3], Xiaodong Zhang[2,3], Cuixia Zhang[2,3], Shuqun Song[4]

[1] Institute of Marine Science and Technology, Shandong University, 27 Shanda Nan Road, Jinan 250110, PR China

[2] Tianjin Key Laboratory of Marine Resources and Chemistry, Tianjin University of Science and Technology, Tianjin 300457, PR China

[3] College of Marine and Environmental Sciences, Tianjin University of Science and Technology, Tianjin 300457, PR China

[4] CAS Key Laboratory of Marine Ecology and Environmental Sciences, Institute of Oceanology, Chinese Academy of Sciences, Qingdao 266071, PR China

Correspondence to: Jun Sun (phytoplankton@163.com)

Abstract. We studied the biodiversity of autotrophic calcareous coccolithophore assemblages at 30 locations in the Eeastern Eequatorial Indian Ocean (EEIO) (80°-94°E, 6°N-5°S) and evaluated the importance of regional hydrology. We found 25 taxa We documented 25 taxa and 17 taxa based on identification of coccospheres and coccoliths, respectively.of coccospheres and 17 taxa of coccoliths. The coccolithophore community was dominated by *Gephyrocapsa oceanica*, *Emiliania huxleyi*, *Florisphaera profunda*, *Umbilicosphaera sibogae*, and *Helicosphaera carteri*. The abundance of coccoliths and coccospheres ranged from 0.192×10^3 to 161.709×10^3 coccoliths l^{-1} and 0.192×10^3 to 68.365×10^3 cells l^{-1}, averaged at 22.658×10^3 coccoliths l^{-1} and 9.386×10^3 cells l^{-1}, respectively. Biogenic PIC, POC, and rain ratio mean values were 0.498 μgC l^{-1}, 1.047 μgC l^{-1}, and 0.990 respectively. High abundances of both coccoliths and coccospheres in the surface ocean layer occurred north of the equator. Vertically, the great majority of coccoliths and coccospheres were concentrated in water less than 75 m deep. The ratios between the number of coccospheres and free coccoliths across four transects indicated a pattern that varied among different oceanographic settings. The *H'* and *J* values of coccospheres were similar compared with those of coccoliths. Abundant coccolithophores along the equator mainly occurred west of 90°E, which was in accordance with the presence of Wyrtki jets (WJs). And specific - species patterns indicated typical hydrography. *F. profunda* was not found in surface water, indicating a stratified and stable water system. *U. irregularis* dominated in the equatorial zone, suggesting oligotrophic water conditions. Coccosphere distribution was explained by environmental variables, indicated by multi-dimensional scaling (MDS) ordination in response variables and principal components analysis (PCA) ordination in explanatory variables. Coccolithophore distribution was related to temperature, salinity, density and chlorophyll *a*.

1 Introduction

The Indian Ocean is the world's third largest ocean basin, and it is strongly influenced by the South Asian monsoon system. The warm seawater area in the eastern equatorial Indian Ocean (EEIO) is a large region that influences worldwide climatology and El Niño/Southern Oscillation (ENSO) events (Zhang et al., 2009; Peng et al., 2015). The Indian Ocean dipole is another oceanic phenomenon influencing global oceanographic circulation (Horii et al., 2009). Surface currents in the EEIO are diverse and seasonally dynamic due to monsoon forces. Unlike other ocean basins, the Indian Ocean experiences prevailing semiannual currents (Luyten and Roemmich, 1982; Zhang, 2015). Many currents prevail in the EEIO during the summer and winter monsoon periods. These include the Equatorial undercurrent and the South Java Current (Iskandar, 2009; Peng et al., 2015). There are also currents that exist throughout the year. One example is the Indonesian throughflow (ITF), which is the passageway connecting the Pacific Ocean and Indian Ocean (Ayers et al., 2014). In the spring and fall intermonsoon periods, many surface circulations disappear, and Wyrtki jets (WJs) are the only semi-annual currents present at the equator. The equatorial Indian Ocean is controlled by the eastward WJs (also known as Equatorial Jets) (Wang, 2015).

Living coccolithophores thrive in the photic water column. Coccolithophores are unicellular microalgal flagellates with diverse life cycles (alternating diploid - haploid stage) belonging to marine nanoplankton (Moheimani et al., 2012; Taylor et al., 2016).– Life phase transitions can easily occur in natural assemblages when nutrient level changed (Taylor et al., 2017).They generate external calcified scales (coccoliths) responsible for large areas of visible "white water" recorded by satellite remote sensing. The coccolithophore cell is surrounded by several thin layers of coccoliths. Coccolithophores are globally distributed and contribute up to 10% of the global phytoplankton biomass (Holligan et al., 1983; Brown and Yoder, 1994; Guptha et al., 2005; Sadeghi et al., 2012; Hagino and Young, 2015; Oviedo et al., 2015). This calcareous nanoflora usually dominates the open ocean plankton community (O'Brien et al., 2013; Sun et al., 2014). In its dual functions of biomineralization and photoautotrophy, the coccolithophore community influences the global carbon cycle, sulphur cycle and oceanographic parameters (Sun, 2007; Taylor et al., 2017). Inorganic calcareous coccoliths can serve as a physical ballast for organic carbon sequestration in the deep ocean (Ziveri et al., 2007; Bolton et al., 2016; Rembauville et al., 2016). As a consequence, the PIC/POC (particulate inorganic carbon to organic carbon = "rain ratio"), is a factor explaining biomineralization process impacts on organic production exports. Coccolithophore assemblages are sensitive to climate variability (Tyrrell, 2008; Silva et al., 2013). Increased CO_2 concentrations combined with other factors (e.g., nutrient elements, pH, irradiance, temperature) stimulated cell organic carbon fixation (photosynthesis) have diminished the rain ratio of coccolithophores (Feng et al., 2008; Langer et al., 2009; Riebesell et al., 2000; Shi et al., 2009;). These calcifying nanoplankton is negatively affected by ocean acidification with decreased carbonate availability especially in colder water realm (Oviedo et al., 2017; Smith et al., 2017). Herein, the response of coccolithophore ecophysiology to environmental change has aroused a big concern (Poulton et al., 2017). The coccolithophore cell (coccosphere) is surrounded by several thin layers of coccoliths, When detached coccoliths were exported to the deep sediment, whichthey provided an ideal tool to are useful in reconstructing paleoenvironmental changepaleoceanographic history, e.g. sea-surface temperature, mixed layer and nutricline (Ferreira et al., 2017; Guerreiro et al., 2013; Guptha et al., 2005; Laprida et al., 2017). Coccolithophore geographical distributions interact with environment conditions, thus making them useful in paleoenvironmental reconstructions (Laprida et al., 2017). Coccolithophore community structure and ecological distributions in the Atlantic Ocean have been documented by McIntyre et al., (1970), Brown and Yoder, (1994), Baumann et al., (1999), Kinkel et al., (2000), and Shutler et al., (2013). Pacific Ocean studies have included McIntyre et al., (1970), Okada and Honjo, (1973, 1975), Honjo and Okada, (1974), Okada and McIntyre, (1977), Houghton and Guptha, (1991), Saavedra-Pellitero, (2011), Saavedra-Pellitero et al., (2014), and López-Fuerte et al., (2015). Most of the coccolithophore studies were limited to surface waters.

The Indian Ocean is the world's third largest ocean basin, and it is strongly influenced by the South Asian monsoon system. The warm seawater area in the eastern equatorial Indian Ocean (EEIO) is a large region that influences worldwide climatology and El Niño/Southern Oscillation (ENSO) events (Zhang et al., 2009; Peng et al., 2015). The Indian Ocean dipole is another oceanic phenomenon influencing global oceanographic circulation (Horii et al., 2009). Surface currents in the EEIO are diverse and seasonally dynamic due to monsoon forces. Unlike other ocean basins, the Indian Ocean experiences prevailing semiannual currents (Luyten and Roemmich, 1982; Zhang, 2015). Many currents prevail in the EEIO during the summer and winter monsoon periods. These include the Equatorial undercurrent and the South Java Current (Iskandar, 2009; Peng et al., 2015). There are also currents that exist throughout the year. One example is the Indonesian throughflow (ITF), which is the passageway connecting the Pacific Ocean and Indian Ocean (Ayers et al., 2014). In the spring and fall intermonsoon periods, many surface circulations disappear, and Wyrtki jets (WJs) are the only semi-annual currents present at the equator. The equatorial Indian Ocean is controlled by the eastward WJs (also known as Equatorial Jets) (Wang, 2015).

Studies on coccolithophores in the Indian Ocean have been relatively recent compared to Atlantic and Pacific Ocean studies. Coccolithophore studies in the Indian Ocean mainly include Young (1990), Giraudeau and Bailey (1995), Broerse et al. (2000), Lees (2002), Andruleit (2007), Mohan et al. (2008), Mergulhao et al. (2013), in regard to nanofossil or living species biogeography in the monsoon season. Relatively few studies have evaluated the occurrence of living coccolithophores in the water column during the intermonsoon period in the eastern Indian Ocean. Our three main objectives were to (1) document the abundance, diversity and geographical patterns of living coccolithophores; (2) explain variations occurring in the nanoflora assemblages; (3) correlate these variations to regional hydrographic parameters.

2 Materials and methods

2.1 Survey area and sampling strategy

An initial investigation cruise was conducted in the eastern equatorial Indian Ocean (EEIO) (80°~94°E, 6°N~5°S) (Fig. 1) onboard R/V "*Shiyan* 1" from March 10th through April 9th, 2012. Seawater ~~samples (400-500 mL) and chlorophyll *a* (Chl*a*) samples were~~was collected at seven depths from the surface to 200 m using Niskin bottles on a rosette sampler (Sea-Bird SBE-911 Plus V2). At all the stations, temperature and salinity profile data were determined in situ with the attached sensors system (conductivity-temperature-depth, CTD).

2.2 ~~Phytoplankton~~ Coccolithophore analysis

Coccolithophore samples were filtered 400-500 ml with a mixed cellulose membrane (25 mm, 0.22 μm) using a Millipore filter system connected to a vacuum pump under < 20 mm Hg filtration pressure. After room temperature drying in plastic Petri dishes, the filters were cut and subsequently mounted on glass slides with neutral balsam for polarized microscope (Motic, BA300POL.) examination (Sun et al., 2014). Totally at least 400 fields was counted by the standard of 30 coccospheres and 50 coccoliths enumerated. The coccolithophore abundance was finally calculated following the formula in Sun et al. (2014).

2.3 Size-fractionated Chl*a* analysis

~~Chl*a*~~ Chlorophyll *a* (Chl*a*) samples were serially filtered 800 ml using the same filtration system (vacuum < 200 mm Hg) through 20 μm × 20 mm silk net (micro-class), 2 μm × 20 mm nylon membrane (nano-class) and 0.7 μm × 20 mm Whatman GF/F filters (pico-class). After filtration, Chl*a* membranes were immediately wrapped in aluminum foil and stored in a freezer -20℃ freezer. In the laboratory, Chl*a* measurements were made using the fluorescence method of Parsons et al. (1984).

2.4 Estimation of coccolith calcite, coccosphere carbon biomass

The cell size biovolume was evaluated from geometric models (Sun and Liu, 2003) and then converted into carbon biomass (i.e. coccolithophore organic carbon, ~~POC,~~ particulate organic carbon, POC, hereafter) using the formula of Eppley et al. and Guo et al. (Eppley et al., 1970; Guo et al., 2016). Determinations of calcite-$CaCO_3$ (i.e. coccolithophore inorganic carbon, particulate inorganic carbon, PIC, hereafter~~PIC, particulate inorganic carbon~~) masses were based on k_s values (shape factor) and length maximum (diameter, μm) recorded in previous studies (Young and Ziveri, 2000; Yang and Wei, 2003). The PIC/POC value is a potential rain ratio, which expresses the carbonate flux export to the outside of the euphotic water. Seawater samples were filtered one liter for qualitative diagnosis under scanning electron microscope (SEM). As for the irregularly shaped coccolithophores whose biovolume has rare records, nearly 33% of the species were estimated with geometric models using SEM pictures from the literature, websites, and this study (Kleijne, 1991; Giraudeau and Bailey, 1995; Cros and Fortuño, 2002; Young et al., 2003). The website can be visited via the access: http://ina.tmsoc.org/Nannotax3/index.html. It is noted that organic carbon was calculated with the exception of *Gladiolithus flabellatus* and *Reticulofenestra sessilis* by the reason of insufficient records in SEM.

2.5 Multivariate analysis

The spatial distribution of coccolithophores and hydrologic data were analyzed using freeware package Ocean Data View (ODV) 4.7.6 (https://odv.awi.de/en/). Box-whisker plots were prepared by the Golden Software Grapher (LLC, Colorado, USA) 10.3.825. Cluster analysis and non-metric multidimensional scaling (Shen et al., 2010) on coccosphere data (after square root transformation) were simultaneously implemented using the program package PRIMER 6.0 (Plymouth Routines In

MultivariateEcological Research, developed at the Plymouth Marine Laboratory, United Kingdom). Prior to the above operations, the raw data were square root transformed. Then, principal component analysis (PCA) considering Euclidean distance was employed after data transformation and normalization. Significance testing was performed using the Analysis of Similarities (ANOSIM) analysis. The Similarity Percentages-Species Contributions the Similarity Percentages Routine (SIMPER) program was used for evaluating the contribution of each species to their sample group. All analyses were conducted to visualize the relations between phytoplankton abundance data and specific environmental factors.

3 Results

3.1 Hydrographic features

The present investigation area crossed diverse hydrographic gradients as seen from the profile temperature and salinity (vertical temperature and salinity data not shown). Temperature increased southwards along longitudinal section (Fig. 2a). Notably, there was a interesting phenomenon at St. I306 with lowest temperature and highest salinity. High temperature and highly saline waters from the west equatorial zone were advected into the east equatorial zone (Fig. 2a, b). The temperature-salinity (T-S) curve had an inverted-L-shape (Fig. 2c). During the spring monsoon transition period, the water column was well stratified and quite stable, which is mainly attributed to weak wind-driven surface circulation compared to the monsoon period ~~(vertical temperature and salinity data not shown)~~. Due to the well stratified water column, the spring intermonsoon was considered to be the most oligotrophic period (Rixen et al., 1996).

3.2 Taxonomic composition and characteristics

Samples of living coccolithophores from the EEIO during the spring intermonsoon period yielded 26 species, representing 25 taxa of coccospheres and 17 taxa of coccoliths. ~~Scanning electron microscope (~~SEM~~)~~ photographs of selected species are shown in Plates I-VI, including several predominant taxa. Among coccolith ~~species~~, *Gephyrocapsa oceanica*, *Emiliania huxleyi*, *Umbilicosphaera sibogae*, *Helicosphaera carteri*, and *H. hyalina* were most dominant. Coccosphere assemblages were dominanted by*G. oceanica*, *Florisphaera profunda*, *E. huxleyi*, *Umbellosphaera irregularis*, and *U. sibogae*. *G. oceanica* was overwhelmingly dominant among the coccoliths, with frequency and relative abundance up to 96.5% and 71.76%, respectively. The rest of coccolith ~~species~~ were similar in frequency and abundance. *G. oceanica* and *E. huxleyi* had high frequencies, with 44.5% and 31%, respectively. *F. profunda* had the highest (up to 40.78%) relative abundance (Fink et al., 2010).

Coccolith and coccosphere density ranged from 0.192×10^3 to 161.709×10^3 coccoliths $l^{-1}$and 0.192×10^3 to 68.365×10^3 cells l^{-1}, averaged at 22.658×10^3 coccoliths l^{-1} and 9.386×10^3 coccoliths l^{-1}, respectively. The most predominant coccolith ~~species~~ *G. oceanica* was ranged ~154.955×10^3 coccoliths l^{-1}, with a mean value of 16.260×10^3 coccoliths l^{-1}. And the most predominant coccosphere ~~species~~ was still represented by *G. oceanica*, whose abundance ranged ~24.805×10^3 cells l^{-1}, with average value 2.458×10^3 cells l^{-1}. The abundances of five dominant coccolith and five taxa of coccosphere ~~species~~ are shown in Fig. 3. The other dominant coccoliths had similar abundances. For the remaining coccosphere ~~species~~, *G. oceanica* and *U. irregularis* were more abundant than *E. huxleyi* and *U. sibogae*.

3.3 Distribution and diversity pattern

The horizontal distributions of dominant coccoliths and coccospheres are shown in Fig. 4 and Fig. 5. Coccolith abundance was greatest in three regions: south of Sri Lanka, easternmost Sri Lanka, and southernmost area (Fig. 4). There was a peculiar oceanographic phenomenon at St. I316 characterized by surface lowest temperature and highest salinity, where the coccoliths of *U. sibogae* and *H. carteri* were predominantly occupied (Fig. 4). Abundance was relatively low in the equatorial region. In contrast to the coccoliths, coccospheres were more homogeneous in their horizontal distributions (Fig. 5).

Dominant coccolithophores abundances along two sections are illustrated in Figs. 6~9. More abundant coccolith ~~species~~ were restricted to the water column west of 90°E (Fig. 6). Nearly no coccoliths were distributed from the surface down to 50 m along east of 90°E. Dominant coccospheres abundance in section A were mainly represented by *F. profunda* and *U. irregularis* (Fig. 7). These two taxa followed trends similar to the coccoliths. For section B, coccolith abundance was primarily contributed by~~due to~~ *G. oceanica* (Fig. 8) and abundance was concentrated in the easternmost region. *E. huxleyi* and *U. sibogae* were mainly distributed in deeper water. *H. hyalina* abundance decreased in deeper and open water and *H. carteri* showed a plaque pattern. Fig. 9 shows obvious coccosphere abundance in the 75 m water layer of section B, where a deep abundance maximum was located. *F. profunda* was the dominant coccosphere in the assemblage at section B.

Vertically, ~~numerous~~ The dominant coccoliths were confined to the middle layer (25 m-75 m) in the EEIO (Fig. 10). ~~The~~ Most of them~~others~~ reached peak values at the 50 m water layer, except for *E. huxleyi* and *H. carteri*, whose peak values were located in the 200 m and 100 m water layers. Coccosphere ~~species~~ increased from the surface towards the middle water, and then decreased towards the bottom water (Fig. 11). The ratios between coccospheres and free coccoliths were charted along transects (Fig. 12). The ratio values basically coincided with coccosphere abundance. The ratio reached a maximum in the 40 m layer along sections A and C. The ratio along section B exhibited a differed trend and its maximum was at the surface layer. The section D ratio was concurrent with the section C ratio.

3.4 Estimation of PIC, POC, and rain ratios

The mean PIC, POC, and rain ratios were 0.498 μgC l^{-1}, 1.047 μgC l^{-1}, and 0.990, respectively. The surface distributions and depth-integrated patterns of PIC, POC, and rain ratio are shown in Fig. 13. We found a dominance of *Oolithotus fragilis* and *G. oceanica* in biogenic PIC. Unlike PIC, POC was mainly contributed by cells of *U. sibogae* and *U. irregularis*. The pattern of PIC and POC appeared to be similar. The surface water of the inner and outer of Sri Lanka section displayed two peaks. In the case of the integral value, PIC and POC were preferentially distributed west of the equator. The depth averaged-rain ratio peak occurred at 80°E-85°E.

In section A, *O. fragilis*contributed about 48% of total PIC, with a maximum value at Station (St.) I405 accounting for 94%. The POC distribution pattern was similar to *U. irregularis* abundance. The maximum rain ratio value occurred east of the equator. In section B, PIC was represented by *F. profunda*. POC and cell abundance showed concurrent trends. Rain ratio had a clear pattern with higher values in the surface and bottom layers.

3.5 Coccosphere clustering and analysis

Coccosphere samples at 75 m layer (Deep Chlorophyll Maximum, DCM), where great quantities of coccosphere located, were chosen for the cluster and MDS analysis. The combinations of clustering technique and MDS method are usually conductive to obtain balanced and reliable conclusions in ecological studies (Liu, 2015;Clarke and Warwick, 2001). All samples could be clustered into four groups (Group a, b, c, d). MDS stress values (0.15) lesser than 0.2 give an useful ordination picture, particularly at the lower end of this range (Cox and Cox, 1992;Clarke and Warwick, 2001). ANOSIM analysis revealed remarkable difference (Global R=0.85, p=0.001) among group classification with the exception of Group b-d and Group c-d whose R value < p value (Fink et al., 2010). It is accepted that Global R value larger than 0.5 accounts for significant difference among groups (Liao, 2013). Apparently, localities were basically classified along transects (e.g. Group c included the equatorial localities), whereas some exceptions existed (Fig. 14). Besides, MDS bubble plots for first six dominant coccosphere ~~species~~ were presented in Fig. 14. It is apparently that, Group a and b were mainly composed by dominant coccosphere *G. oceanica*, *F. profunda* ~~and~~, *E. huxleyi* and *A. robusta*. While Group c was primarily contributed by species *U. sibogae* and *U. irregularis*. Considering Group d only contained two localities, *G. oceanica* dominated the whole group. The SIMPER results were shown in Table 4. It showed the contribution rates of dominant coccosphere in each group.

4 Discussion

4.1 Coccolithophore species diversity and distributions in the EEIO

The surface water of eastern Sri Lanka (around St. I 104A) had the greatest coccolith and coccosphere ~~species~~ richness and abundance. The biodiversity indices were much lower around the neighboring waters of Sri Lanka (Fig. 15), suggesting that the local water in that system lacked ecosystem stability. The *H'* and *J* coccospheres values were slightly higher compared with coccolith values (Fig. 16). Therefore, coccosphere aggregations exhibited more diversity than coccoliths. This finding was consistent with that of Guptha et al. (2005). The physical distributions of coccolithophore assemblages in relation to the temperature-salinity are also shown (Figs. 17, 18). The coccoliths represented by *G. oceanica*, *U. sibogae*, *H. carteri* and *H. hyalina* were concentrated in the surface layer characterized by high temperature and low salinity and the bottom euphotic layer characterized by low temperature and high salinity. ~~Conversely~~Besides, *E. huxleyi* was predominantly distributed in the intermediate layer with moderate temperature and salinity. The coccospheres, *F. profunda* and *E. huxleyi* were mainly found in the deeper euphotic layer where the DCM layer is located. *U. irregularis* and *U. sibogae* had greater abundances in the surface layer, confirming their preference for oligotrophic conditions. There was a peculiar oceanographic phenomenon at St. I316 characterized by surface lowest temperature and highest salinity, where the coccoliths of *U. sibogae* and *H. carteri* were predominantly occupied (Fig.

4). *F. profunda* was only distributed below 50 m at St. I316, indicating a stratified and stable water locally. In other words, this peculiar hydrology was not caused by vertical upwelling, maybe water mass advection instead. It is very hard to identify what kinds of currents created this peculiar biophysical distribution, after all water currents are not prosperous during intermonsoon period.

The POC pattern can be represented by coccosphere abundance. Varied allocation to calcification produced dissimilarities in the PIC/POC ratios. Large rain ratio values around the Sri Lanka waters predicted a mineral ballast with a drawdown of biological carbon towards the deep seafloor (Iglesias-Rodriguez et al., 2008; Findlay et al., 2011). We suggest that the rain ratio (Zondervan et al., 2002) is of great importance in predicting biominerolization and photosynthetic production (Bolton et al., 2016).

4.2 Coccolithophore ecological preferences

Many coccolithophore indicator species were collected in this study although several were uncommon. *G. oceanica* is a representative dominant species that shows preference for eutrophic water (Andruleit et al., 2000). In the surface distribution of *G. oceanica*, both coccoliths and coccospheres were predominantly distributed in the easternmost waters of Sri Lanka. This may be due to the ~~nutrients~~eutrophic water derived from the highly productive Andaman Sea which was linked to the Bay of Bengal through narrow channels (Gibson et al., 2007; Nielsen et al., 2004). The coccosphere of *U. irregularis* was only common in the equatorial zone, indicating oligotrophic water conditions there (Kleijne et al., 1989). In the Indian Ocean, eight species of *Florisphaera* were discovered in deep water (Kahn and Aubry, 2012). We found only one species of *Florisphaera* (*F. profunda*) and it typically occurred in the disphotic layer below 100 m. As an inhabitant of deep water, *F. profunda* hardly occurred in~~was not found~~ in surface water layer unless with the appearance of vertical upwelling~~, indicating a stratified and stable water system~~. The coccoliths of *U. sibogae* and *H. carteri* maxima were found at St. I316 indicating that these species showed affinities to low temperature and high salinity water. The cosmopolitan taxa, *Calcidiscus leptoporus*, was detected and its coccoliths peaked at a depth of 200 m at St. I705. *C. leptoporus* is sparsely distributed in the water column, whereas it predominates in the coccolithophore flora of the sediment owing to its resistance to disintegration (Renaud et al., 2002). The ratios between the number of coccospheres and free coccoliths across four transects were separately demonstrated and the vertical distribution patterns were variable. This level of biogeographic variation might be related to regional hydrographic features. We presumed that coccospheres disintegrated into coccoliths after sinking for a certain distance at section B. Different circumstances appeared at section A, where a subsurface coccosphere maximum at the 40 m layer occurred. This finding coincided with the pattern of biological abundance. Ratios in sections C and D were consistent with ratios observed in the equator section (Monechi et al., 2000).

4.3 Factors regulating coccolithophore assemblage structure

Coccolithophore abundance was relatively low during the low wind transition period compared to previous studies conducted during the monsoon period in the EEIO. The low abundance is due to the gentle winds and low nutrient availability during the spring intermonsoon season leading to low primary productivity and biomass in the EEIO (Morrison et al., 1998). The surface coccolithophores were most abundant in the northeastern area where pockets of low-salinity water plume occur (Fig. 2). This resulted from the inflow of less saline water into the equatorial Indian Ocean from the Bay of the Bengal and Andaman Seas (Wyrtki, 1961; LaViolette, 1967). The outflows derived from the surface water of the Andaman Sea become concentrated between the south Nicobar Islands and Sumatra (Rizal et al., 2012). In contrast, a highly saline water tongue was observed along the equatorial Indian Ocean (west of 90°E), indicating that Wyrtki jets (WJs) prevailed during the spring intermonsoon period. There was consistency in the ~~nanofloral~~ coccolithophore distribution pattern at the equator (section A, Figs. 6, 7). The maximum abundance along west of 90°E was probably caused by inflow from WJs considering their ability to alter the oceanic layer structure. PCA was carried out to examine the relationships among the environmental variables (Fig. 19). Coccolithophore abundance was driven primarily by temperature, salinity, density~~ and Chl*a*~~. As a phytoplankton group, coccolithophore abundance usually corresponded to Chl*a* content in the sea. The cluster of environmental data from sample locations coincided with the grouping of species data (except for a few isolated points). The most abundant species is shown above each locality symbol. The first three principal components (PC1, PC2, PC3) were extracted based on eigenvalues larger than 1 and explain 42%, 24%, and 20.2% of the variation, respectively. The cumulative variances of the three components reached up to 86.2% (PC3 not shown). The eigenvectors of all five principal components are shown in Table 5. The results of PCA indicated that salinity, density, and pico-Chl*a* had a positive relation with PC1, whereas a close correlation occurred in Group B that was dominated by *E. huxleyi* and *G. oceanica*. Similarly, temperature, Chl*a*, micro-Chl*a* and nano-Chl*a* were positively correlated to PC2. Groups C and D, characterized by *U. irregularis*, were associated with temperature. The majority of localities in Group A (represented by *F. profunda*) were negatively related to Chl*a* and size-fractionated Chl*a*. Finally, the MDS ordination of coccosphere abundance and the PCA ordination of environmental variables are in good agreement. This high degree of matching in our study confirmed that the present explanatory variables (Tezel and Hasırcı, 2013) are appropriate for explaining the biological response variables.

5 Conclusions

The coccolithophore assemblage in the EEIO during the spring intermonsoon season was primarily comprised of the coccoliths *G. oceanica*, *E. huxleyi*, *U. sibogae*, *H. carteri*, and *H. hyalina* and the coccospheres *G. oceanica*, *F. profunda*, *E. huxleyi*, *U. irregularis*, and *U. sibogaes*. The abundance of coccoliths and coccospheres ranged from 0.192×10^3 ~ 161.709×10^3 coccoliths l^{-1} and 0.192×10^3 ~ 68.365×10^3 cells l^{-1}, with an average value of 22.658×10^3 coccoliths l^{-1} and 9.386×10^3 cells l^{-1}, respectively. The mean values of biogenic PIC, POC, and the rain ratio were 0.498 μg C l^{-1}, 1.047 μg C l^{-1}, and 0.990, respectively. The rain ratio was considered to be of great importance so relative biovolume and carbon biomass were calculated. Additional studies using direct chemical treatments on coccoliths and coccospheres might establish a relationship between biovolume conversion and chemical measurements and provide more accurate data.

The horizontal distributions of coccolithophores exhibited three patches: south of Sri Lanka, easternmost Sri Lanka, and southernmost area. An unusual phenomenon was observed at the surface water of St. I316. Vertically, coccoliths abundance were restricted to the water column west of 90°E, exactly consistent with WJs appearance.

The localities and coccosphere species were ordered by MDS and all samples were clustered into four groups in the EEIO. The coccolithophore abundance in this study was relatively low and resulting from the weak winds and minimal nutrient upwelling compared to previous studies that were conducted during the summer or winter monsoon seasons. During the spring intermonsoon period, no significant oceanic circulation occurred in the EEIO except for WJs. We inferred that, in the study area, different coccolithophore species had specific environmental preferences. Thus, coccolithophore species are good indicators of oceanographic changes in the EEIO. PCA was used to study the correlation among environmental variables, indicating positive or negative relationships with nanofloral species. Coccosphere distribution was highly correlated to specific environmental variables. This was shown by the MDS ordination of response variables and PCA ordination of explanatory variables. Coccolithophores can be used as dynamic indicators of the upper ocean for their sensitivity to environmental changes. Obtaining knowledge of specific cellular physiological behavior related to global change variables will be a future challenge. We attempted to evaluate coccolithophore POC contents using a carbon-volume model that was subject to a degree of error. Future planned studies will involve indoor experiments using axenic cultures of coccolithophores. The cell POC will be measured using advanced chemical techniques. Carbon evaluation of the field community will then be compared with direct measurements from controlled laboratory experiments.

Acknowledgements. We wish to thank the Dr. Dongxiao Wang and Dr. Yunkai He for providing and processing CTD dataset. Dr. Ying Wang, Bing Xue and Xiaoqian Li were also appreciated for their constructive comments on the paperwork. This work was supported by the Natural Science Foundation of China (41276124) andNational Basic Research Program of China (2015CB954002), Science Fund for University Creative Research Groups in Tianjin (TD12-5003), and the Program for Changjiang Scholars to Jun Sun. It was also partly supported by the Natural Science Foundation of China (41676112, 41306119, 41306118). The Captain and Crews of R/V *Shiyan1* were acknowledged for their assistance in sample collection during the cruise, and the Open Cruises from the Natural Science Foundation of China. We also thank LetPub (www.letpub.com) for its linguistic assistance during the preparation of this manuscript.

References

Andruleit, H.: Status of the Java upwelling area (Indian Ocean) during the oligotrophic northern hemisphere winter monsoon season as revealed by coccolithophores, Mar. Micropaleontol., 64, 36-51, doi:10.1016/j.marmicro.2007.02.001, 2007.

Andruleit, H. A., von Rad, U., Brans, A., and Ittekkot, V.: Coccolithophore fluxes from sediment traps in the northeastern Arabian Sea off Pakistan, Mar. Micropaleontol., 38, 285-308, doi: 10.1016/s0377-8398(00)00007-4, 2000.

Ayers, J. M., Strutton, P. G., Coles, V. J., Hood, R. R., and Matear, R. J.: Indonesian throughflow nutrient fluxes and their potential impact on Indian Ocean productivity, Geophys. Res. Lett., 41, 5060-5067, doi: 10.1002/2014GL060593, 2014.

Baumann, K. H., Cepek, M., and Kinkel, H.: Coccolithophores as indicators of ocean water masses, surface-water temperature, and paleoproductivity—examples from the South Atlantic, in: Use of Proxies in Paleoceanography, 117-144, Springer, doi10.1007/978-3-642-58646-0_4, 1999.

Bolton, C. T., Hernández-Sánchez, M. T., Fuertes, M.-Á., González-Lemos, S., Abrevaya, L., Mendez-Vicente, A., Flores, J.-A., Probert, I., Giosan, L., and Johnson, J.: Decrease in coccolithophore calcification and CO_2 since the middle Miocene, Nat. Commun., 7, doi: 10.1038/ncomms10284, 2016.

Broerse, A., Brummer, G.-J., and Van Hinte, J.: Coccolithophore export production in response to monsoonal upwelling off Somalia (northwestern Indian Ocean), Deep-Sea Res. Pt. II: Topical Studies in Oceanography, 47, 2179-2205, 2000.

Brown, C., and Yoder, J.: Distribution pattern of coccolithophorid blooms in the western North Atlantic Ocean, Cont. Shelf Res., 14, 175-197, 1994.

Clarke, K. R., and Warwick, R.M.: Change in marine communities: an approach to statistical analysis and interpretation, Plymouth, UK: Primer E, 2001.

Cox, M. A., and Cox, T.: Interpretation of Stress in non-metric multidimensional scaling, Statistica Applicata, 4, 611-618, 1992.

Cros, L., and Fortuño, J. M.: Atlas of northwestern Mediterranean coccolithophores, Sci. Mar., 66, 1-182, 2002.

Eppley, R. W., Reid, F., and Strickland, J.: Estimates of phytoplankton crop size, growth rate, and primary production, Calif. Univ. Scripps Inst. Oceanogr. Bull., 1970.

Feng, Y., Warner, M. E., Zhang, Y., Sun, J., Fu, F.-X., Rose, J. M., and Hutchins, D. A.: Interactive effects of increased pCO2, temperature and irradiance on the marine coccolithophore *Emiliania huxleyi* (Prymnesiophyceae), Eur. J. Phycol., 43, 87-98, doi: 10.1080/09670260701664674, 2008.

Ferreira, J., Mattioli, E., and Van de Schootbrugge, B.: Palaeoenvironmental vs. evolutionary control on size variation of coccoliths across the Lower-Middle Jurassic, Palaeogeogr. Palaeocl., 465, 177-192, doi: 10.1016/j.palaeo.2016.10.029, 2017.

Findlay, H. S., Calosi, P., and Crawfurd, K.: Determinants of the PIC: POC response in the coccolithophore *Emiliania huxleyi* under future ocean acidification scenarios, Limnol. and Oceanogr., 56, 1168-1178, doi:10.4319/lo.2011.56.3.1168, 2011.

Fink, C., Baumann, K.-H., Groeneveld, J., and Steinke, S.: Strontium/Calcium ratio, carbon and oxygen stable isotopes in coccolith carbonate from different grain-size fractions in South Atlantic surface sediments, Geobios, 43, 151-164, 10.1016/j.geobios.2009.11.001, 2010.

Gibson, R. N., Atkinson, R. J. A., & Gordon, J. D. M.: Coral reefs of the Andaman Sea—an integrated perspective. Oceanography and Marine Biology: An Annual Review, 45, 173-194, doi: 10.1201/9781420050943.ch5, 2007.

Giraudeau, J., and Bailey, G. W.: Spatial dynamics of coccolithophore communities during an upwelling event in the Southern Benguela system, Cont. Shelf Res., 15, 1825-1852, doi:10.1016/0278-4343(94)00095-5, 1995.

Guerreiro, C., Oliveira, A., De Stigter, H., Cachão, M., Sá, C., Borges, C., Cros, L., Santos, A., Fortuño, J.-M., and Rodrigues, A.: Late winter coccolithophore bloom off central Portugal in response to river discharge and upwelling, Cont. Shelf Res., 59, 65-83, doi: 10.1016/j.csr.2013.04.016, 2013.

Guo, S., Sun, J., Zhao, Q., Feng, Y., Huang, D., and Liu, S.: Sinking rates of phytoplankton in the Changjiang (Yangtze River) estuary: A comparative study between Prorocentrum dentatum and Skeletonema dorhnii bloom, J. Marine Syst., 154, 5-14, doi: 10.1016/j.jmarsys.2015.07.003, 2016.

Guptha, M. V. S., Mergulhao, L. P., Murty, V. S. N., and Shenoy, D. M.: Living coccolithophores during the northeast monsoon from the Equatorial Indian Ocean: Implications on hydrography, Deep-Sea Res. Pt II, 52, 2048-2060, doi:10.1016/j.dsr2.2005.05.010, 2005.

Hagino, K., and Young, J. R.: Biology and Paleontology of Coccolithophores (Haptophytes), in: Marine

Protists, Springer, 311-330, 2015.
Holligan, P., Viollier, M., Harbour, D., Camus, P., and Champagne-Philippe, M.: Satellite and ship studies of coccolithophore production along a continental shelf edge, Nature, 304, 339-342, doi:10.1038/304339a0, 1983.
Honjo, S., and Okada, H.,: Community structure of coccolithophores in the photic layer of the mid-Pacific, Micropaleontology, 209-230, doi: 10.2307/1485061, 1974.
Horii, T., Masumoto, Y., Ueki, I., Hase, H., and Mizuno, K.: Mixed layer temperature balance in the eastern Indian Ocean during the 2006 Indian Ocean dipole, J. Geophys. Res.: Oceans, 114, doi:10.1029/2008JC005180, 2009.
Houghton, S. D., and Guptha, M. S.: Monsoonal and fertility controls on recent marginal sea and continental shelf coccolith assemblages from the western Pacific and northern Indian oceans, Mar. Geol., 97, 251-259, doi:10.1016/0025-3227(91)90119-O, 1991.
Iglesias-Rodriguez, M. D., Halloran, P. R., Rickaby, R. E., Hall, I. R., Colmenero-Hidalgo, E., Gittins, J. R., Green, D. R., Tyrrell, T., Gibbs, S. J., and von Dassow, P.: Phytoplankton calcification in a high-CO_2 world, Science, 320, 336-340, doi: 10.1126/science.1154122 2008.
Iskandar I, Masumoto Y, and Mizuno K.: Subsurface equatorial zonal current in the eastern Indian Ocean, J.Geophys. Res., 114, 1-12, doi: 10.1029/2008JC005188, 2009.
Kahn, A., and Aubry, M.-P.: New species of the coccolithophore *Florisphaera* Okada and Honjo 1973, Micropaleontology, 58, 209-215, 2012.
Kinkel, H., Baumann, K.-H., and Cepek, M.: Coccolithophores in the equatorial Atlantic Ocean: response to seasonal and Late Quaternary surface water variability, Mar. Micropaleontol., 39, 87-112, doi:10.1016/S0377-8398(00)00016-5, 2000.
Kleijne, A., Kroon, D., and Zevenboom, W.: Phytoplankton and foraminiferal frequencies in northern Indian Ocean and Red Sea surface waters, Neth. J. Sea Res., 24, 531-539, doi:10.1016/0077-7579(89)90131-2, 1989.
Kleijne, A.: Holococcolithophorids from the Indian Ocean, Red Sea, Mediterranean Sea and North Atlantic Ocean, Mar. Micropaleontol., 17, 1-76, doi:10.1016/0377-8398(91)90023-Y, 1991.
López-Fuerte, F. O., Gárate-Lizárraga, I., Siqueiros-Beltrones, D. A., and Yabur, R.: First record and geographic range extension of the coccolithophore *Scyphosphaera apsteinii* Lohman, 1902 (Haptophyta: Pontosphaeraceae) from the Pacific coast of Mexico, Check List, 11, 1754, doi: http://dx.doi.org/10.15560/11.5.1754, 2015.
Langer, G., Nehrke, G., Probert, I., Ly, J., and Ziveri, P.: Strain-specific responses of Emiliania huxleyi to changing seawater carbonate chemistry, Biogeosciences, 6, 2637-2646, doi:10.5194/bg-6-2637-2009, 2009.
Laprida, C., Chapori, N. L. G., and Violante, R. A.: Principles of paleoceanographic reconstruction, in: The Argentina Continental Margin, 71-90, Springer International Publishing, 2017.
LaViolette, P. E.: Temperature, salinity, and density of the world's seas: Bay of Bengal and Andaman Sea, DTIC Document, 1967.
Lees, J. A.: Calcareous nannofossil biogeography illustrates palaeoclimate change in the Late Cretaceous Indian Ocean, Cretaceous Res., 23, 537-634, doi:10.1006/cres.2003.1021, 2002.
Liao, X. L., Chen, P. M., Ma, S. W., Chen, H. G.: Community structure of phytoplankton and its relationship with environmental factors before and after construction of artificial reefs in Yangmeikeng, Daya Bay, South China Fisheries Science, 9, 109-119, doi: 10. 3969/ j. issn. 2095 - 0780. 2013. 05. 017, 2013.

Liu, H. J., Sun, J., Feng, Y. Y.: Study on modern coccolithophores in coastal region along the east Hainan Island, Haiyang Xuebao, 37, 27-40, doi: 10.3969/j.issn.0253-4193.2015.12.004, 2015.

Luyten, J. R., and Roemmich, D. H.: Equatorial currents at semi-annual period in the Indian Ocean, J. Phys. Oceanogr., 12, 406-413, doi: http://dx.doi.org/10.1175/1520-0485(1982)012<0406:ECASAP>2.0.CO;2 1982.

McIntyre, A., Bé, A., and Roche, M.: Modern Pacific Coccolithophorida: a paleontological thermometer, Transactions of the New York Academy of Sciences, 32, 720, doi: 10.1111/j.2164-0947.1970.tb02746.x, 1970.

Mergulhao, L. P., Guptha, M., Unger, D., and Murty, V.: Seasonality and variability of coccolithophore fluxes in response to diverse oceanographic regimes in the Bay of Bengal: Sediment trap results, Palaeogeography, Palaeoclimatology, Palaeoecology, 371, 119-135, doi: http://dx.doi.org/10.1016/j.palaeo.2012.12.024, 2013.

Mohan, R., Mergulhao, L. P., Guptha, M., Rajakumar, A., Thamban, M., AnilKumar, N., Sudhakar, M., and Ravindra, R.: Ecology of coccolithophores in the Indian sector of the Southern Ocean, Mar. Micropaleontol., 67, 30-45, doi:10.1016/j.marmicro.2007.08.005, 2008.

Moheimani, N. R., Webb, J. P., and Borowitzka, M. A.: Bioremediation and other potential applications of coccolithophorid algae: A review, Algal Res., 1, 120-133, doi:10.1016/j.algal.2012.06.002, 2012.

Monechi, S., Buccianti, A., and Gardin, S.: Biotic signals from nanoflora across the iridium anomaly in the upper Eocene of the Massignano section: evidence from statistical analysis, Mar. Micropaleontol., 39, 219-237, 2000.

Morrison, J., Codispoti, L., Gaurin, S., Jones, B., Manghnani, V., and Zheng, Z.: Seasonal variation of hydrographic and nutrient fields during the US JGOFS Arabian Sea Process Study, Deep-Sea Res. Pt II: Topical Studies in Oceanography, 45, 2053-2101, doi:10.1016/S0967-0645(98)00063-0, 1998.

Nielsen, T. G., Bjørnsen, P. K., Boonruang, P., Fryd, M., Hansen, P. J., Janekarn, V., Limtrakulvong, V., Munk, P., Hansen, O. S., Satapoomin, S., Sawangarreruks, S., Thomsen, H. A., and Østergaard, J. B.: Hydrography, bacteria and protist communities across the continental shelf and shelf slope of the Andaman Sea (NE Indian Ocean). Marine Ecology Progress Series, 274, 69-86, 2004.

~~O'Brien, C., Peloquin, J., Vogt, M., Heinle, M., Gruber, N., Ajani, P., Andruleit, H., Arístegui, J., Beaufort, L., and Estrada, M.: Global marine plankton functional type biomass distributions: coccolithophores, Earth Sys. Sci. Data Discuss, 5, 491-520, doi:10.1594/PANGAEA.785092, 2013.~~

Okada, H., and Honjo, S.: The distribution of oceanic coccolithophorids in the Pacific, Deep-Sea Res., 1973, 355-374,

Okada, H., and Honjo, S.: Distribution of coccolithophores in marginal seas along the western Pacific Ocean and in the Red Sea, Mar. Biol., 31, 271-285, doi: 10.1007/BF00387154, 1975.

Okada, H., and McIntyre, A.: Modern coccolithophores of the Pacific and North Atlantic oceans, Micropaleontology, 23, 1-55, doi: 10.2307/1485309, 1977.

Oviedo, A., Ziveri, P., Álvarez, M., and Tanhua, T.: Is coccolithophore distribution in the Mediterranean Sea related to seawater carbonate chemistry?, Ocean Sci., 11, 13-32, doi:10.5194/os-11-13-2015, 2015.

Oviedo, A. M., Ziveri, P., and Gazeau, F.: Coccolithophore community response to increasing pCO_2 in Mediterranean oligotrophic waters, Estuar. Coast. Shelf S., 186, 58-71, doi: org/10.1016/j.ecss.2015.12.007, 2017.

Peng, S., Qian, Y.-K., Lumpkin, R., Du, Y., Wang, D., and Li, P.: Characteristics of the Near-Surface Currents in the Indian Ocean as Deduced from Satellite-Tracked Surface Drifters. Part I: Pseudo-

Eulerian Statistics, J.Phys. Oceanogr., 45, 441-458, doi: 10.1175/jpo-d-14-0050.1, 2015.
Poulton, A. J., Holligan, P. M., Charalampopoulou, A., and Adey, T. R.: Coccolithophore ecology in the tropical and subtropical Atlantic Ocean: New perspectives from the Atlantic meridional transect (AMT) programme, Prog. Oceanogr., doi.org/10.1016/j.pocean.2017.01.003, 2017.
Rembauville, M., Meilland, J., Ziveri, P., Schiebel, R., Blain, S., and Salter, I.: Planktic foraminifer and coccolith contribution to carbonate export fluxes over the central Kerguelen Plateau, Deep-Sea Res. Pt I: Oceanographic Research Papers, 111, 91-101, doi: http://dx.doi.org/10.1016/j.dsr.2016.02.017, 2016.
Renaud, S., Ziveri, P., and Broerse, A. T.: Geographical and seasonal differences in morphology and dynamics of the coccolithophore Calcidiscus leptoporus, Mar. Micropaleontol., 46, 363-385, doi:10.1016/S0377-8398(02)00081-6, 2002.
Riebesell, U., Zondervan, I., Rost, B., Tortell, P. D., Zeebe, R. E., and Morel, F. M.: Reduced calcification of marine plankton in response to increased atmospheric CO_2, Nature, 407, 364-367, doi:10.1038/35030078, 2000.
Rixen, T., Haake, B., Ittekkot, V., Guptha, M., Nair, R., and Schlüssel, P.: Coupling between SW monsoon-related surface and deep ocean processes as discerned from continuous particle flux measurements and correlated satellite data, J. Geophys. Res.: Oceans, 101, 28569-28582, doi: 10.1029/96JC02420, 1996.
Rizal, S., Damm, P., Wahid, M. A., Sundermann, J., Ilhamsyah, Y., and Iskandar, T.: General circulation in the Malacca Strait and Andaman Sea: a numerical model study, Am. J. Environ. Sci., 8, 479, doi:10.3844/ajessp.2012.479.488, 2012.
Saavedra-Pellitero, M., Baumann, K.-H., Flores, J.-A., and Gersonde, R.: Biogeographic distribution of living coccolithophores in the Pacific sector of the Southern Ocean, Mar. Micropaleontol., 109, 1-20, doi: http://dx.doi.org/10.1016/j.marmicro.2014.03.003, 2014.
Saavedra‐Pellitero, M., Flores, J., Lamy, F., Sierro, F., and Cortina, A.: Coccolithophore estimates of paleotemperature and paleoproductivity changes in the southeast Pacific over the past~ 27 kyr, Paleoceanography, 26, 1-16, doi:10.1029/2009PA001824, 2011.
Sadeghi, A., Dinter, T., Vountas, M., Taylor, B., Altenburg-Soppa, M., and Bracher, A.: Remote sensing of coccolithophore blooms in selected oceanic regions using the PhytoDOAS method applied to hyper-spectral satellite data, Biogeosciences, 9, 2127-2143, doi:10.5194/bg-9-2127-2012, 2012.
Shen, P. P., Tan, Y. H., Huang, L. M., Zhang, J. L., and Yin, J. Q.: Occurrence of brackish water phytoplankton species at a closed coral reef in Nansha Islands, South China Sea, Mar. pollut. Bull., 60, 1718-1725, 10.1016/j.marpolbul.2010.06.028, 2010.
Shi, D., Xu, Y., and Morel, F.: Effects of the pH/pCO_2 control method on medium chemistry and phytoplankton growth, Biogeosciences, 6, 1199-1207, doi:10.5194/bg-6-1199-2009, 2009.
Shutler, J., Land, P., Brown, C., Findlay, H., Donlon, C., Medland, M., Snooke, R., and Blackford, J.: Coccolithophore surface distributions in the North Atlantic and their modulation of the air-sea flux of CO2 from 10 years of satellite Earth observation data, Biogeosciences, 10, 2699-2709, doi:10.5194/bg-10-2699-2013, 2013.
Silva, A., Brotas, V., Valente, A., Sá, C., Diniz, T., Patarra, R. F., Álvaro, N. V., and Neto, A. I.: Coccolithophore species as indicators of surface oceanographic conditions in the vicinity of Azores islands, Estuar. Coast.Shelf S., 118, 50-59, doi: http://dx.doi.org/10.1016/j.ecss.2012.12.010, 2013.
Smith, H. E. K., Poulton, A. J., Garley, R., Hopkins, J., Lubelczyk, L. C., Drapeau, D. T., Rauschenberg, S., Twining, B. S., Bates, N. R., and Balch, W. M.: The influence of environmental variability on the

biogeography of coccolithophores and diatoms in the Great Calcite Belt, Biogeosciences Discussions, 1-35, 10.5194/bg-2017-110, 2017.

Sun, J., and Liu, D.: Geometric models for calculating cell biovolume and surface area for phytoplankton, J. Plankton Res., 25, 1331-1346, doi: 10.1093/plankt/fbg096, 2003.

Sun, J.: Organic carbon pump and carbonate counter pump of living coccolithophorid, Advances in Earth Science, 22, 1231-1239, 2007.

Sun, J., Gu, X. Y., Feng, Y. Y., Jin, S. F., Jiang, W. S., Jin, H. Y., and Chen, J. F.: Summer and winter living coccolithophores in the Yellow Sea and the East China Sea, Biogeosciences, 11, 779-806, doi:10.5194/bg-11-779-2014, 2014.

Taylor, A. R., and Brownlee, C.: Calcification, in: The Physiology of Microalgae, 301-318, Springer International Publishing, 2016.

Taylor, A. R., Brownlee, C., and Wheeler, G.: Coccolithophore cell biology: chalking up progress, Ann. Rev. Mar. Sci., 9, 283-310, doi: 10.1146/annurev-marine-122414-034032, 2017.

Tezel, E. E., and Hasırcı, S.: The relationship between environmental variables and the vertical and horizontal assemblages of phytoplankton in Erfelek Reservoir in Sinop, Turkey, Fundam. Appl. Limnol., 183, 177-188, 2013.

Tyrrell, T.: Calcium carbonate cycling in future oceans and its influence on future climates, J. Plankton Res., 30, 141-156, doi:10.1093/plankt/fbm105, 2008.

Wang, Y., and Cui, F. J.: The structure and seasonal variation of upper-layer currents at central equatorial indian ocean, Oceanologia et Limnologia Sinica, 46, 241-247, doi: 10.11693/hyhz20140500128, 2015.

Wyrtki, K.: Physical oceanography of the southeast Asian waters, Scripps Institution of Oceanography, 1961.

Yang, T., and Wei, K.: How many coccoliths are there in a coccosphere of the extant coccolithophorids? A compilation, Journal of Nannoplankton Research, 25, 7-15, 2003.

Young, J.: Size variation of Neogene Reticulofenestra coccoliths from Indian Ocean DSDP Cores, J. Micropalaeontol., 9, 71-86, doi: 10.1144/jm.9.1.71 1990.

Young, J., Geisen, M., Cros, L., Kleijne, A., Sprengel, C., Probert, I., and Ostergaard, J.: A guide to extant coccolithophore taxonomy, Journal of Nannoplankton Research, Special Issue 1, 2003.

Young, J. R., and Ziveri, P.: Calculation of coccolith volume and it use in calibration of carbonate flux estimates, Deep-Sea Res. Pt II: Topical studies in oceanography, 47, 1679-1700, doi:10.1016/S0967-0645(00)00003-5, 2000.

Zhang, Q., Hou, Y., Qi, Q., and Bai, X.: Variations in the eastern Indian Ocean warm pool and its relation to the dipole in the tropical Indian Ocean, Chinese Journal of Oceanology and Limnology, 27, 640-649, doi: 10.1007/s00343-009-9148-5, 2009.

Zhang, Y., Du Y., Zhang, Y. H., Yang, Y. L.: Asymmetric influences of positive and negative IOD events on salinity transport by the fall Wyrtki Jet along the equatorial Indian Ocean, Journal of Tropical Oceanography, 34, 1-10, doi: 10.11978/2014141, 2015.

Ziveri, P., de Bernardi, B., Baumann, K.-H., Stoll, H. M., and Mortyn, P. G.: Sinking of coccolith carbonate and potential contribution to organic carbon ballasting in the deep ocean, Deep-Sea Res. Pt. II: Topical Studies in Oceanography, 54, 659-675, doi:10.1016/j.dsr2.2007.01.006, 2007.

Zondervan, I., Rost, B., and Riebesell, U.: Effect of CO_2 concentration on the PIC/POC ratio in the coccolithophore *Emiliania huxleyi* grown under light-limiting conditions and different daylengths, J. Exp. Mar. Biol. and Ecol., 272, 55-70, 2002.

Table legends:

Table 1 Living coccolithophores composition in the eastern equatorial Indian Ocean during spring intermonsoon period of 2012.

Table 2 Predominant species abundance in the eastern equatorial Indian Ocean during spring intermonsoon period of 2012.

Table 3 Global test by ANOSIM analysis in coccosphere ~~species~~ matrix.

Table 4 Dominant coccosphere ~~species~~ and their contribution to each group revealed by means of SIMPER analysis.

Table 5 The statistical values by PCA analysis in coccosphere ~~species~~ matrix.

Table 1 Living coccolithophores composition in the eastern equatorial Indian Ocean during spring intermonsoon period of 2012.

Species	Frequency of occurrence (%fi)	Relative abundance(%P)	Dominance degree(Y)
Dominant coccoliths			
Gephyrocapsa oceanica	96.5	71.76	0.6925
Emiliania huxleyi	64.0	8.00	0.0512
Umbilicosphaera sibogae	62.5	6.26	0.0391
Helicosphaera carteri	63.5	3.50	0.0222
Helicosphaera hyalina	61.5	3.02	0.0186
Dominant coccospheres			
Gephyrocapsa oceanica	44.5	26.18	0.2330
Florisphaera profunda	22.0	40.78	0.1794
Emiliania huxleyi	31.0	6.46	0.0400
Umbellosphaera irregularis	15.3	11.75	0.0358
Umbilicosphaera sibogae	30.0	4.05	0.0243

Table 2 Predominant species abundance in the eastern equatorial Indian Ocean during spring intermonsoon period of 2012.

Dominant coccoliths	Min, Max (Mean) Units (coccoliths ml^{-1})
Gephyrocapsa oceanica	-, 154.955 (16.260)
Emiliania huxleyi	-, 23.706 (1.814)
Umbilicosphaera sibogae	-, 29.04 (1.418)
Helicosphaera carteri	-, 7.829 (0.793)
Helicosphaera hyalina	-, 10.307 (0.685)
Dominant coccospheres	Min, Max (Mean) Units (cells ml^{-1})
Gephyrocapsa oceanica	-, 24.805 (2.458)
Florisphaera profunda	-, 53.845 (3.828)
Emiliania huxleyi	-, 20.167 (0.606)
Umbellosphaera irregularis	-, 24.675 (1.103)
Umbilicosphaera sibogae	-, 3.609 (0.381)

Table 3 Global test by ANOSIM analysis in coccosphere ~~species~~ matrix.

Pairwise Tests					
Groups	R Statistic	Significance level %	Possible permutations	Actual permutations	Number >= observed
a, b	0.687	0.1	1961256	999	0
a, c	0.997	0.1	38760	999	0
a, d	0.999	0.8	120	120	1
b, c	0.862	0.2	8008	999	1
b, d	0.989	1.5	66	66	1
c, d	0.906	3.6	28	28	1

Table 4 Dominant coccosphere ~~species~~ and their contribution to each group revealed by means of SIMPER analysis.

Group	Average similarity	Dominant species contribution
Coccospheres		
d	40.49	*Gephyrocapsa oceanica* (99.52)
b	53.78	*Gephyrocapsa oceanica* (40.38); *Emiliania huxleyi* (28.62); *Oolithotus fragilis* (11.63); *Florisphaera profunda*(7.97); *Helicosphaera carteri*(4.18)
c	59.53	*Umbellosphaera irregularis*(43.67); *Umbilicosphaera sibogae*(27.06); *Gephyrocapsa oceanica* (10.28); *Helicosphaera hyaline* (8.07); *Emiliania huxleyi* (5.36)
a	61.21	*Florisphaera profunda*(61.89); *Gephyrocapsa oceanica* (22.20);*Algirosphaera robusta* (7.02)

Table 5 The statistical values by PCA analysis in coccosphere ~~species~~ matrix.

Eigenvectors					
Variable	PC1	PC2	PC3	PC4	PC5
Temperature	-0.423	0.468	0.019	0.302	-0.34
Salinity	0.468	-0.102	0.137	0.311	-0.787
Density	0.459	-0.455	0.084	-0.016	0.163
Chl*a*	0.42	0.488	0.089	0.241	0.305
Micro	0.307	0.413	-0.284	-0.755	-0.251
Nano	0.202	0.348	0.682	-0.007	0.199
Pico	0.282	0.186	-0.648	0.429	0.206

Legends:

Fig.1.Study area in the eastern equatorial Indian Ocean showing the station locations.

Fig. 2. Sea surface temperature (°C) and salinity in the surveyed area (left); Temperature-salinity (T-S) diagram in the surveyed area, the blue solid line showed an inversed-L-shape of the hydrologic data (right).

Fig. 3.The abundance of dominant coccolithophore species in the eastern equatorial Indian Ocean. (units: coccoliths l^{-1}, cells l^{-1})

Fig. 4.The surface distribution of dominant coccoliths (units: $\times10^3$ coccoliths l^{-1}) in the surveyed area.

Fig. 5.The surface distribution of dominant coccospheres (units: $\times10^3$ cells l^{-1}) in the surveyed area.

Fig. 6.Dominant coccolith distributions (units: $\times10^3$ coccoliths l^{-1}) along section A of the surveyed area.

Fig. 7.Dominant coccosphere distributions (units: $\times10^3$ cells l^{-1}) along section A of the surveyed area.

Fig. 8.Dominant coccolith distributions (units: $\times10^3$ coccoliths l^{-1}) along section B of the surveyed area.

Fig. 9.Dominant coccosphere distributions (units: $\times10^3$ cells l^{-1}) along section B of the surveyed area.

Fig. 10.Vertical distributions of dominant coccoliths (units: coccoliths l^{-1}) in the surveyed area. (a) Sum; (b) *Gephyrocapsa oceanica*; (c) *Emiliania huxleyi*; (d) *Umbilicosphaera sibogae*; (e) *Helicosphaera carteri*; (f) *Helicosphaera hyaline*

Fig. 11.Vertical distributions of dominant coccospheres (units: cells l^{-1})in the surveyed area. (a) Sum; (b) *Gephyrocapsa oceanica*; (c) *Florisphaera profunda*; (d) *Emiliania huxleyi*; (e) *Umbellosphaera irregularis*; (f) *Umbilicosphaera sibogae*

Fig. 12.The ratio of coccosphere to free coccolith in upper ocean column in the eastern equatorial Indian Ocean. (a): section A; (b): section B; (c): section C; (d): section D

Fig. 13. The horizontal distributions of PIC, POC (units: $\mu gCaCO_3$ l^{-1}, μgC l^{-1}), and rain ratio in the surveyed area. (a)~(c): of surface layer; (d)~(f): of vertically integrated.

Fig. 14 Stations clustered by Bray-Curtis rank similarities and group average linkage (upper); MDS ordination and its bubble plots for six dominant coccosphere ~~species~~ (below).

Fig. 15.Surface distributions of biodiversity index of coccolithophore in the surveyed area.

Fig. 16.Box and whisker diagrams of biodiversity index of coccolithophore in the surveyed area.

Fig. 17.Scatter plots of coccolith distribution under T-S properties in the surveyed area.

Fig. 18.Scatter plots of coccosphere distribution under T-S properties in the surveyed area.

Fig. 19.Ordination biplot based on PCA analysis among environmental variables of the surveyed area. Notes: group partitions here refered to fig. 13; Chla: chlorophyll *a*, Micro: micro-sized Chla, Nano: nano-sized Chla, Pico: Pico-sized Chla, G.o: *Gephyrocapsa oceanica*, F.p: *Florisphaera profunda*,

E.h: *Emiliania huxleyi*, U.i: *Umbellosphaera irregularis*, U.s: *Umbilicosphaera sibogae*, A.r: *Algirosphaera robusta*.

Plate Ⅰ-Ⅵ.

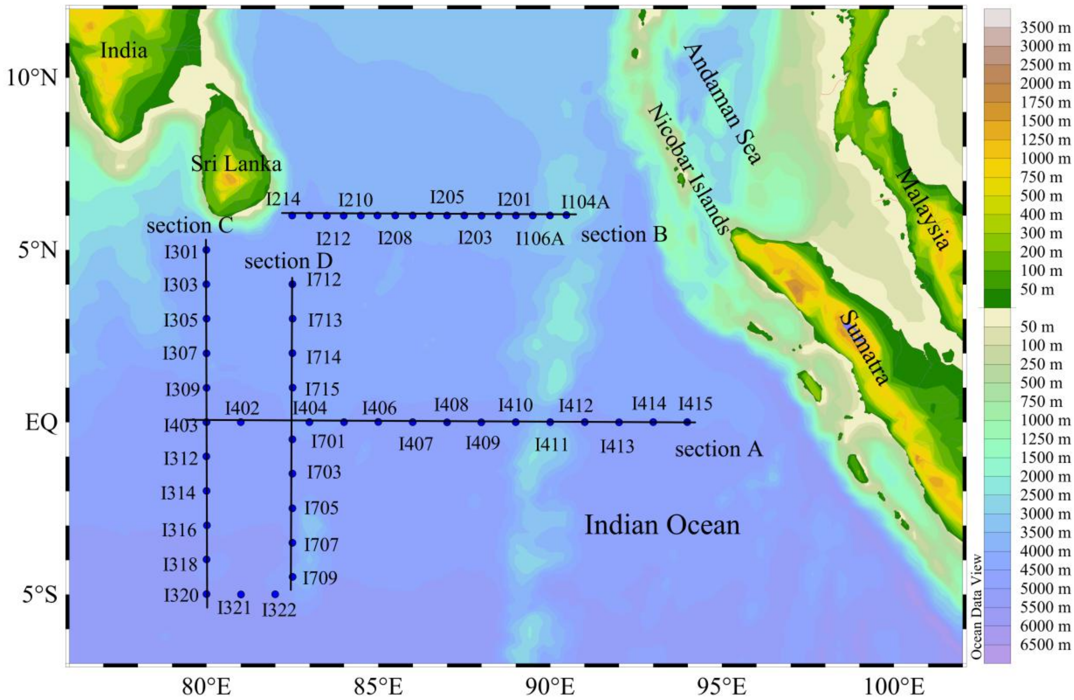

Fig. 1. Study area in the eastern equatorial Indian Ocean showing the station locations.

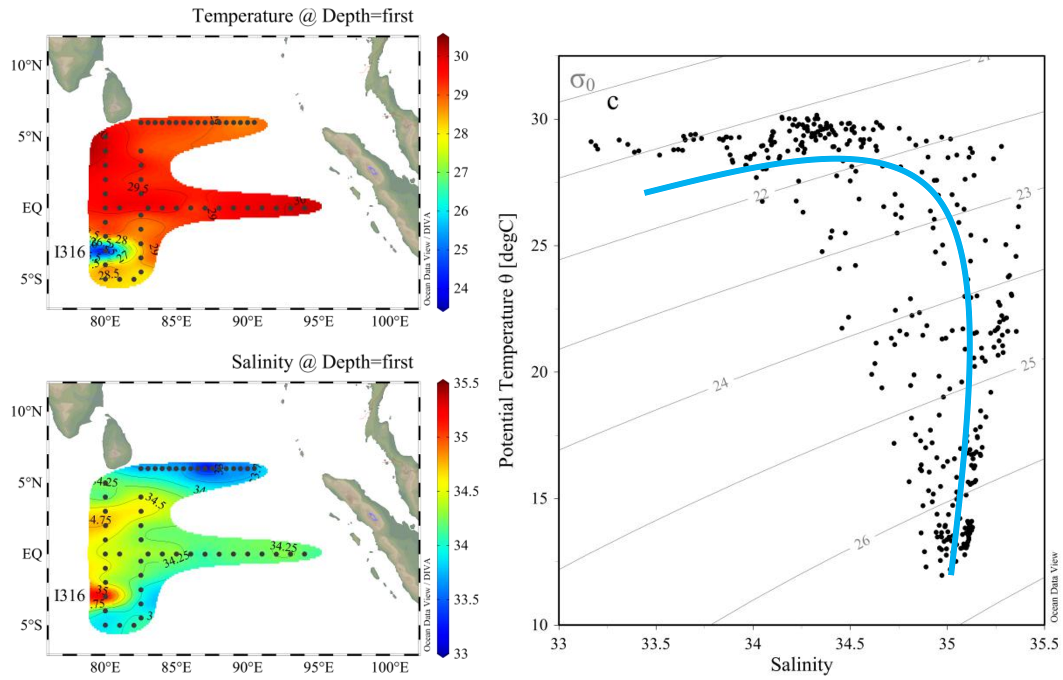

Fig. 2. Sea surface temperature (ºC) and salinity in the surveyed area (left); Temperature-salinity (T-S) diagram in the surveyed area, the blue solid line shows an the inversed-L-shape of the hydrologic data (right).

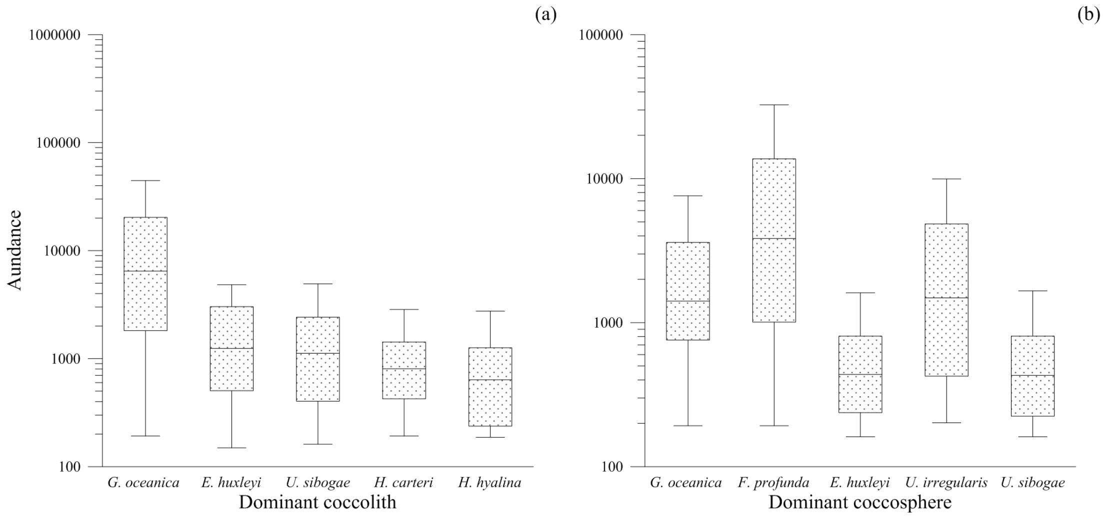

Fig. 3. The abundance of dominant coccolithophore species in the eastern equatorial Indian Ocean. (units: coccoliths l^{-1}, cells l^{-1})

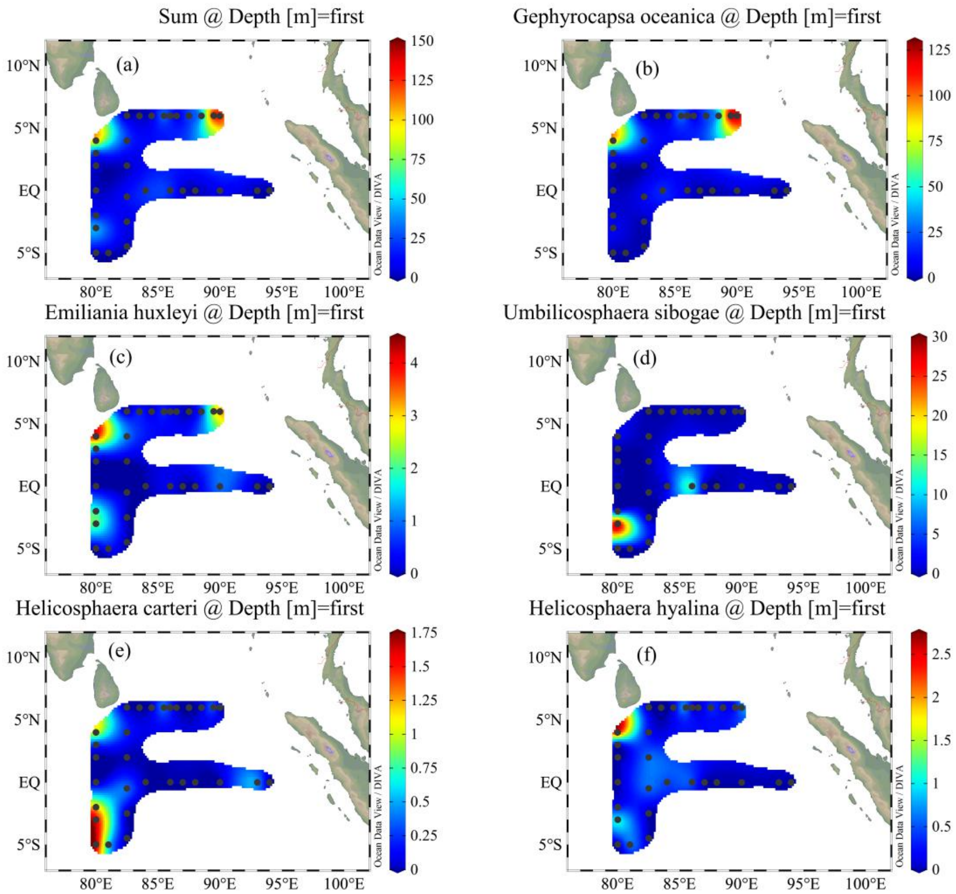

Fig. 4. The surface distribution of dominant coccoliths (units: ×10^3 coccoliths l^{-1}) in the surveyed area.

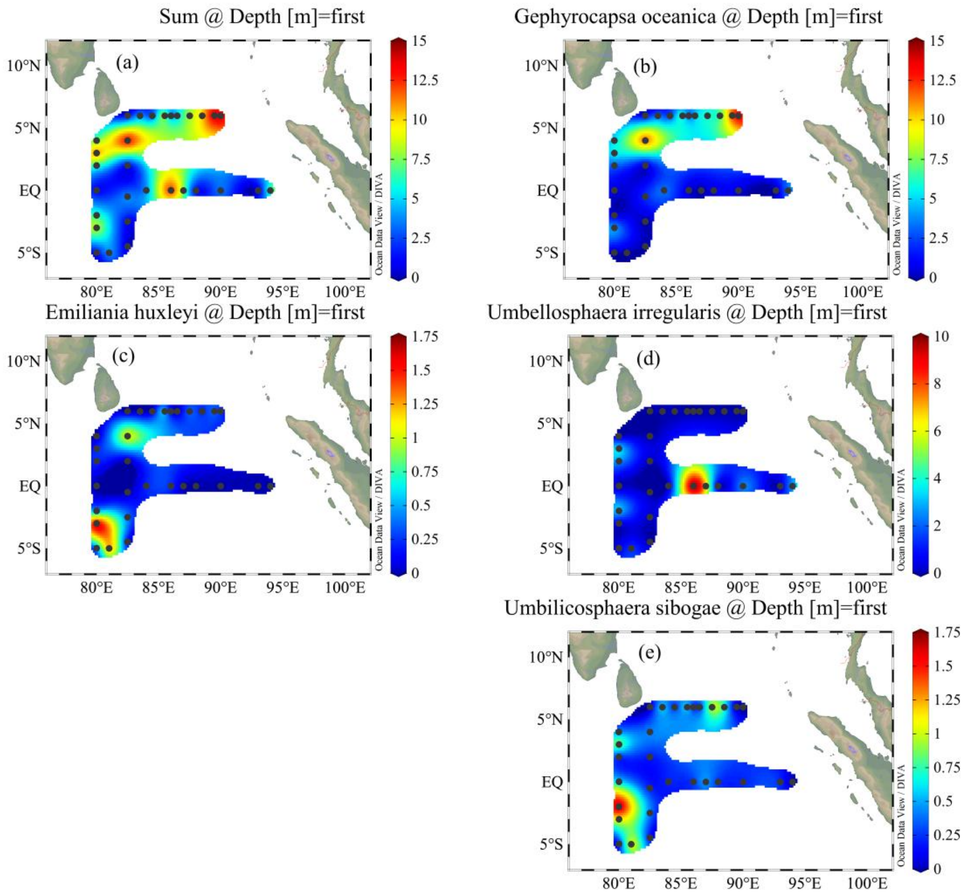

Fig. 5. The surface distribution of dominant coccospheres (units: $\times 10^3$ cells l^{-1}) in the surveyed area.

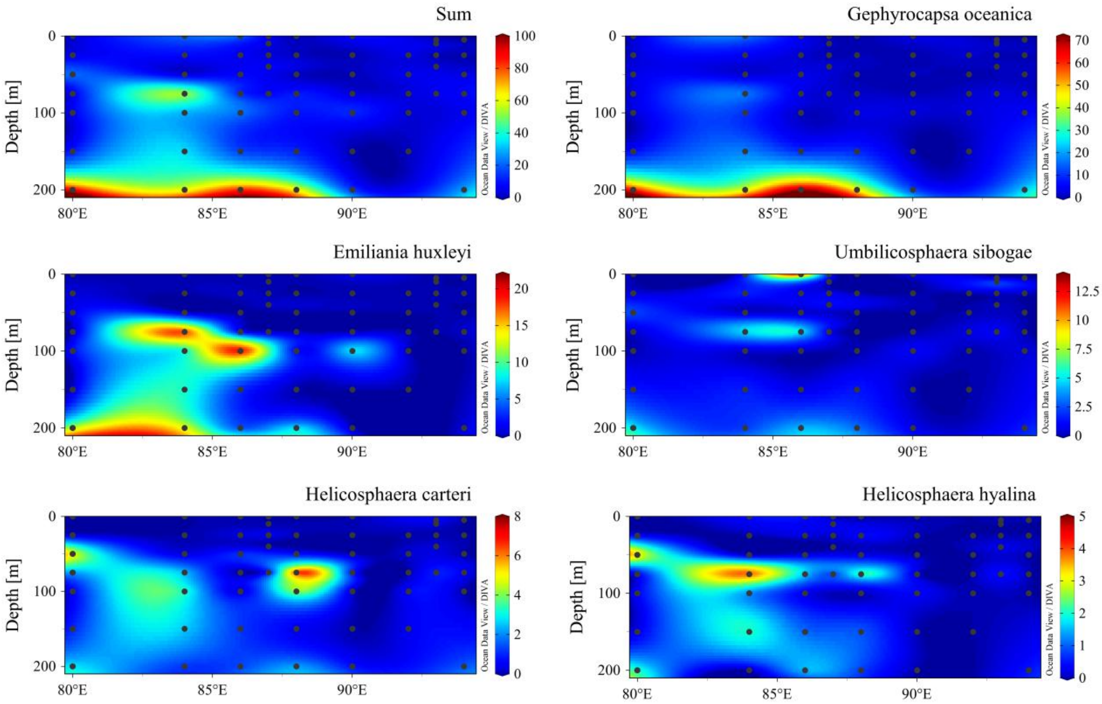

Fig. 6. Dominant coccolith distributions (units: $\times10^3$ coccoliths l^{-1}) along section A of the surveyed area.

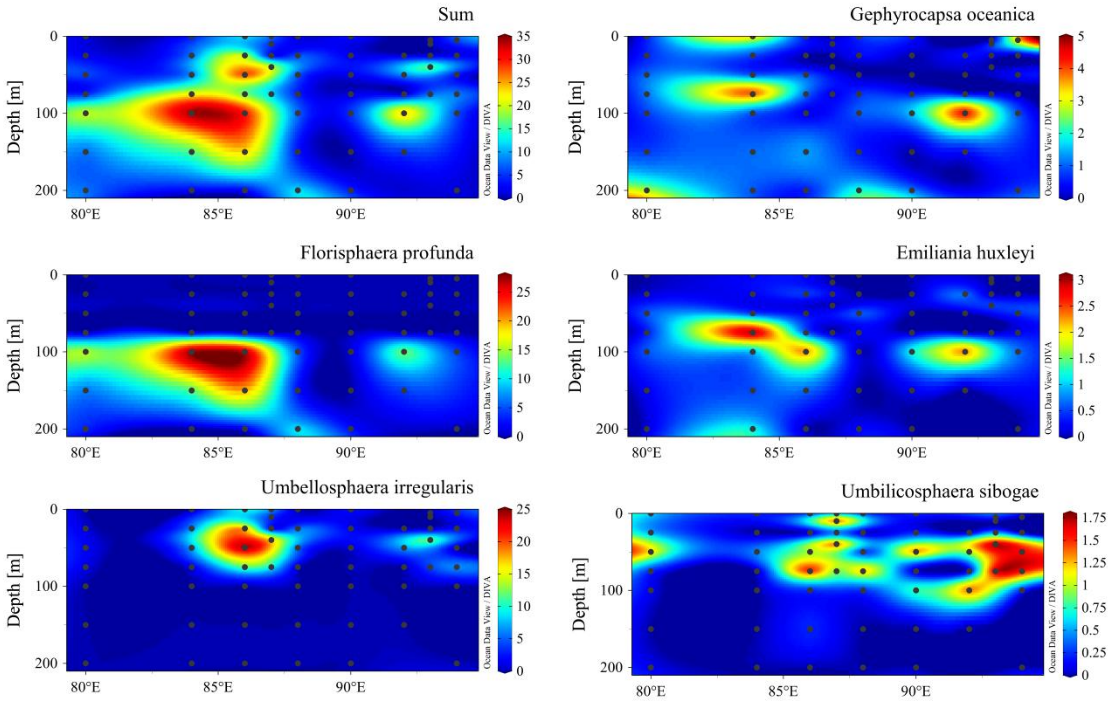

Fig. 7. Dominant coccosphere distributions (units: ×10^3 cells l^{-1}) along section A of the surveyed area.

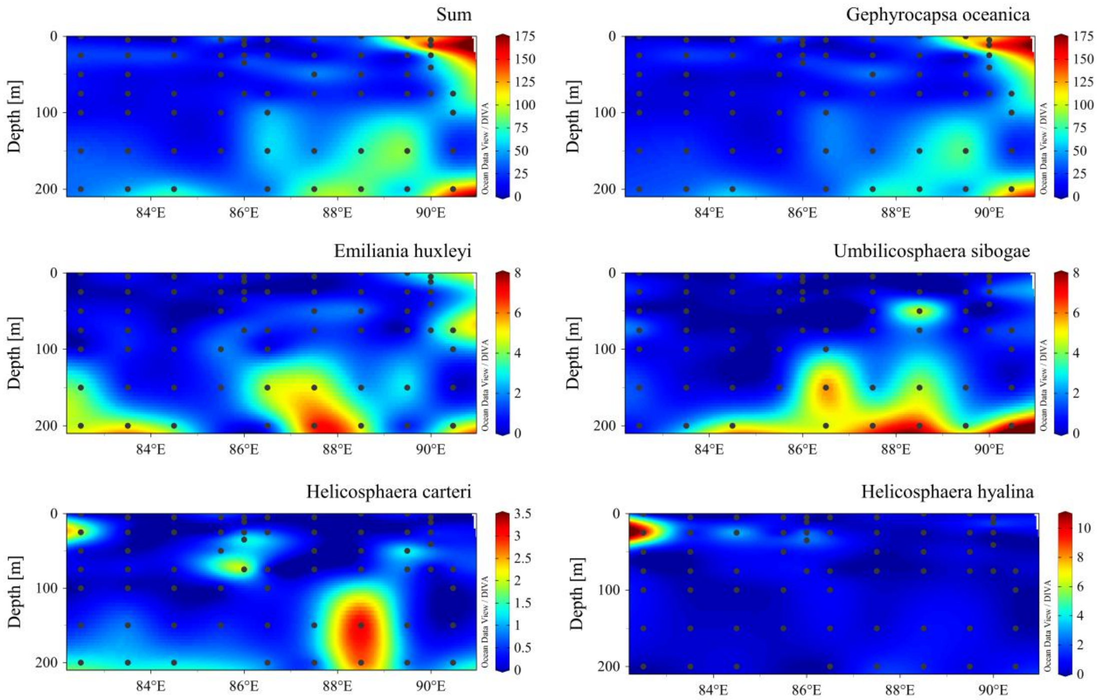

Fig. 8. Dominant coccolith distributions (units: ×10^3 coccoliths l^{-1}) along section B of the surveyed area.

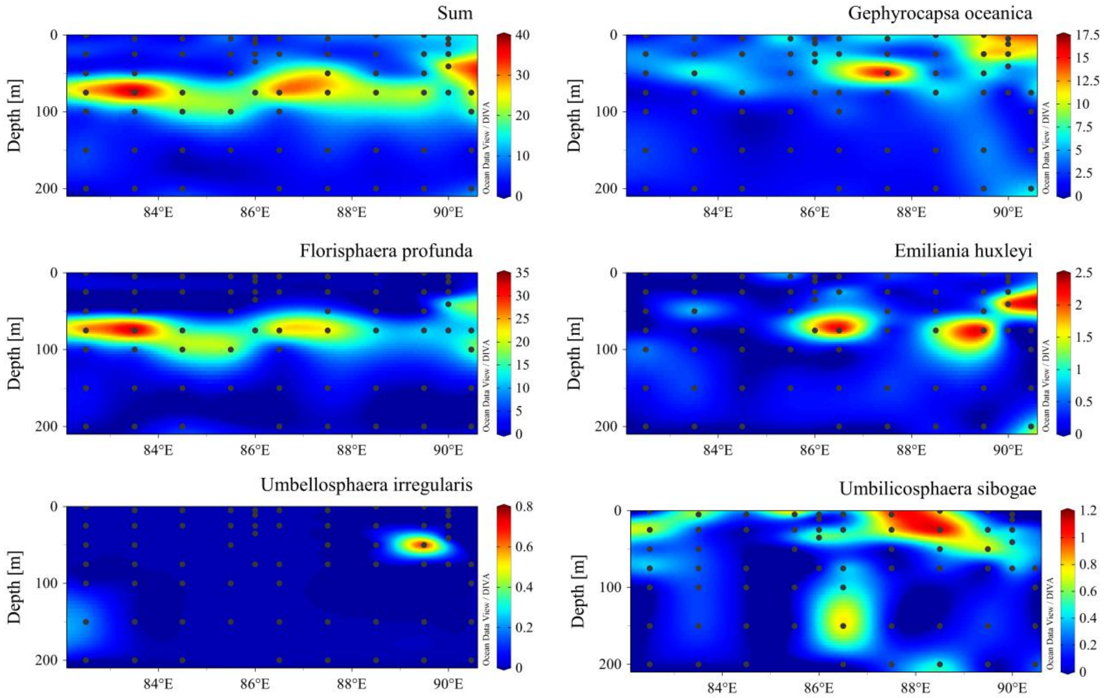

Fig. 9. Dominant coccosphere distributions (units: ×10^3 cells l^{-1}) along section B of the surveyed area.

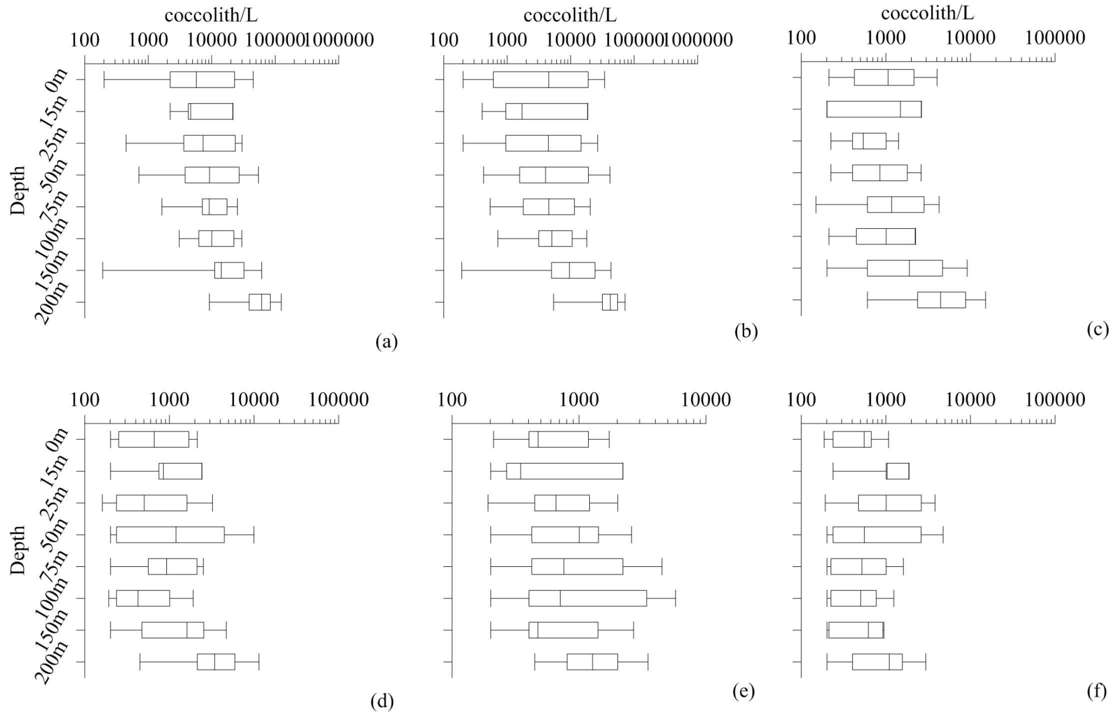

Fig. 10. Vertical distributions of dominant coccoliths (units: coccoliths l^{-1}) in the surveyed area. (a) Sum; (b) *Gephyrocapsa oceanica*; (c) *Emiliania huxleyi*; (d) *Umbilicosphaera sibogae*; (e) *Helicosphaera carteri*; (f) *Helicosphaera hyaline*

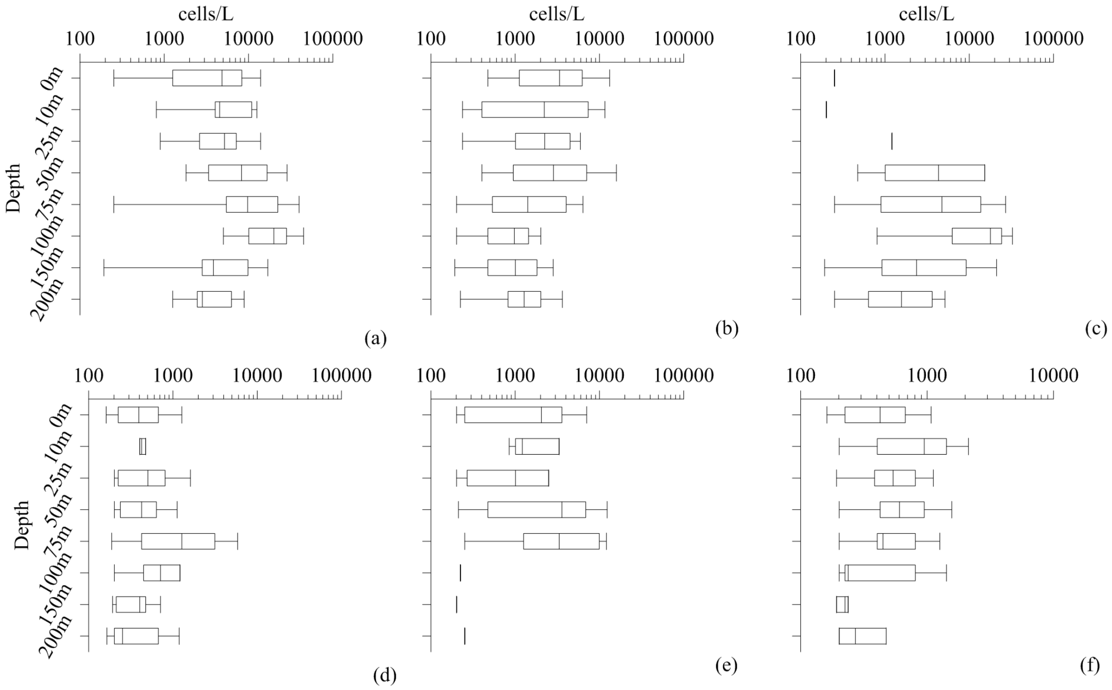

Fig. 11. Vertical distributions of dominant coccospheres (units: cells l^{-1}) in the surveyed area. (a) Sum; (b) *Gephyrocapsa oceanica*; (c) *Florisphaera profunda*; (d) *Emiliania huxleyi*; (e) *Umbellosphaera irregularis*; (f) *Umbilicosphaera sibogae*

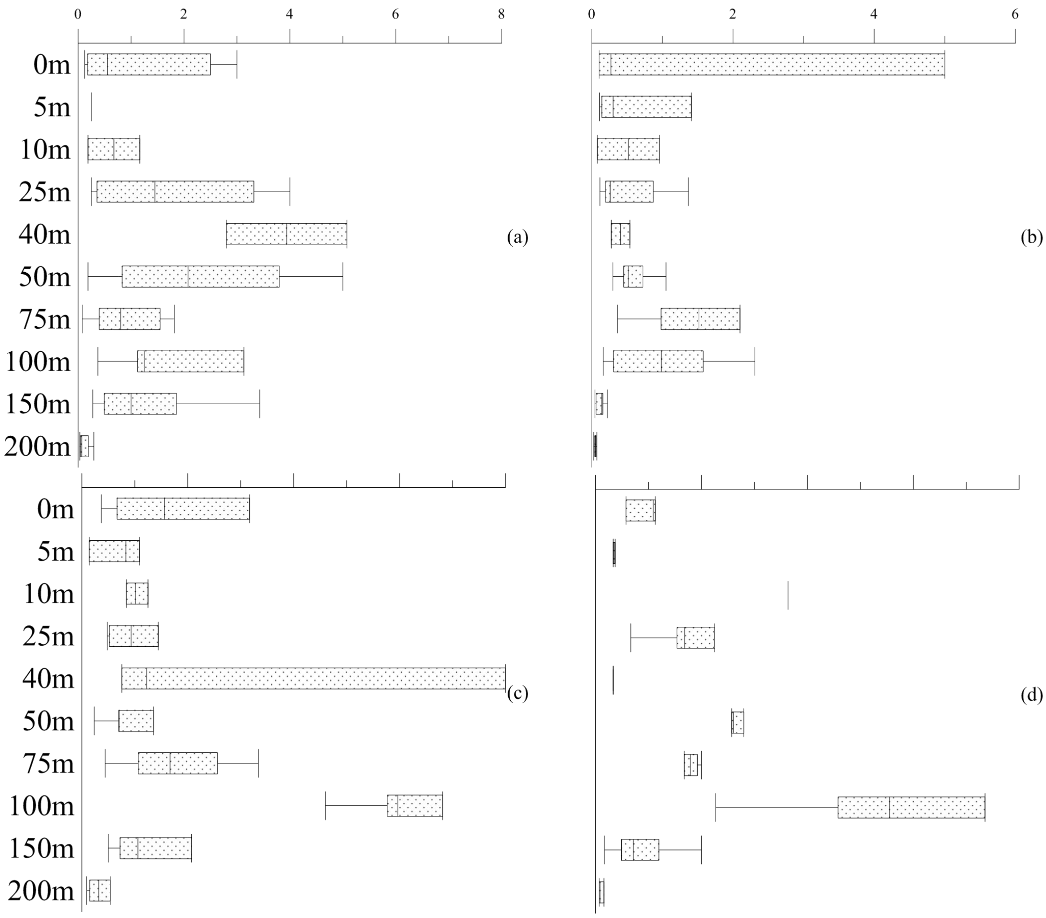

Fig. 12. The ratio of coccosphere to free coccolith in upper ocean column in the surveyed area. (a): section A; (b): section B; (c): section C; (d): section D

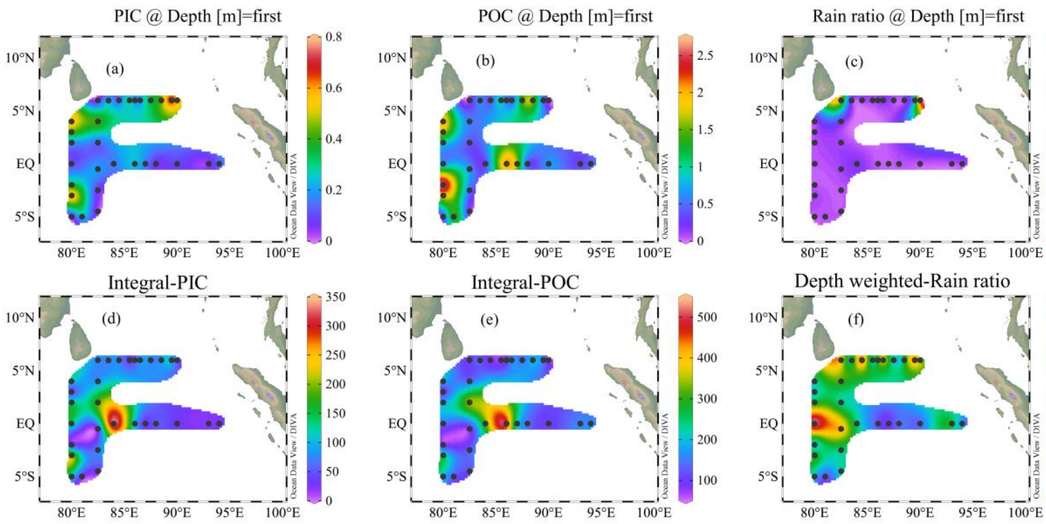

Fig. 13. The horizontal distributions of PIC, POC (units:μgC l^{-1}), and rain ratio in the surveyed area. (a)~(c): of surface layer; (d)~(f): of vertically integrated.

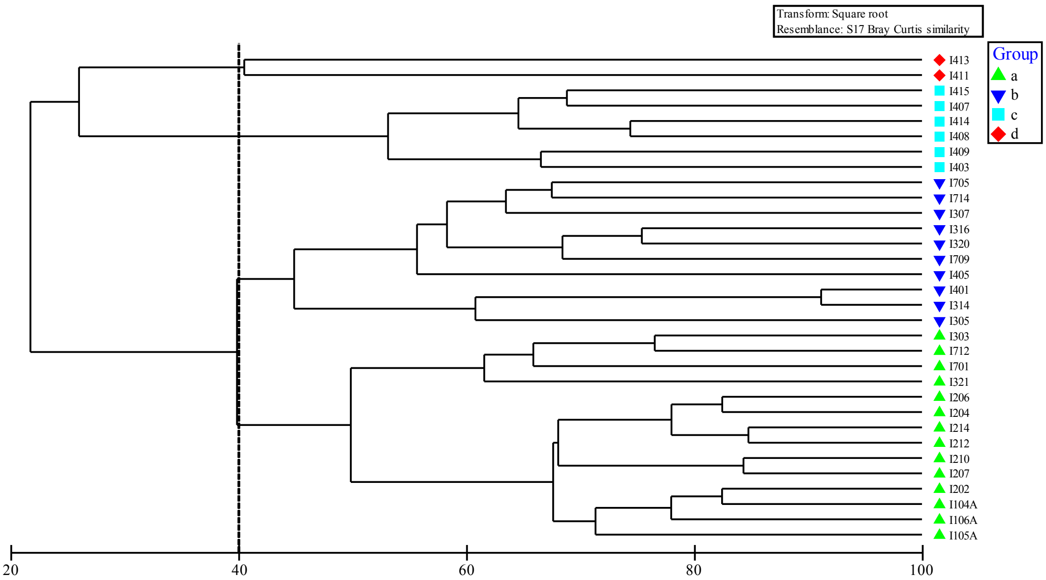
Transform: Square root
Resemblance: S17 Bray Curtis similarity
Group
a
b
c
d
I413
I411
I415
I407
I414
I408
I409
I403
I705
I714
I307
I316
I320
I709
I405
I401
I314
I305
I303
I712
I701
I321
I206
I204
I214
I212
I210
I207
I202
I104A
I106A
I105A
20
40
60
80
100

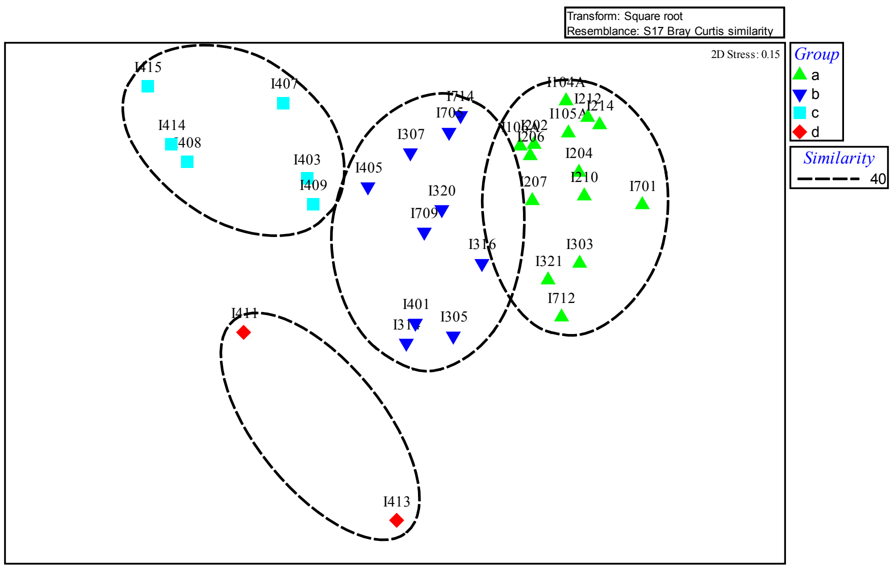
Transform: Square root
Resemblance: S17 Bray Curtis similarity
2D Stress: 0.15
Group
a
b
c
d
Similarity
40

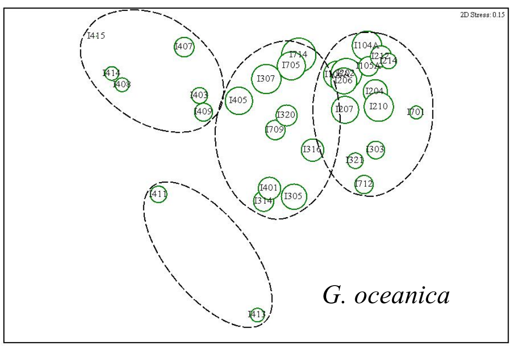
G. oceanica

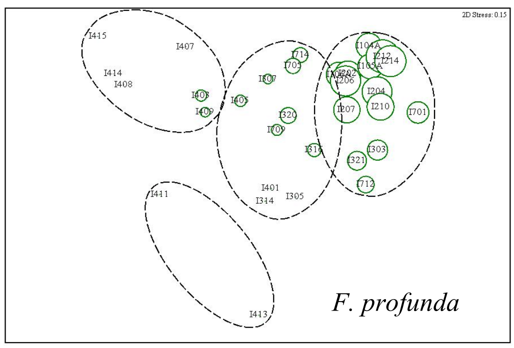
F. profunda

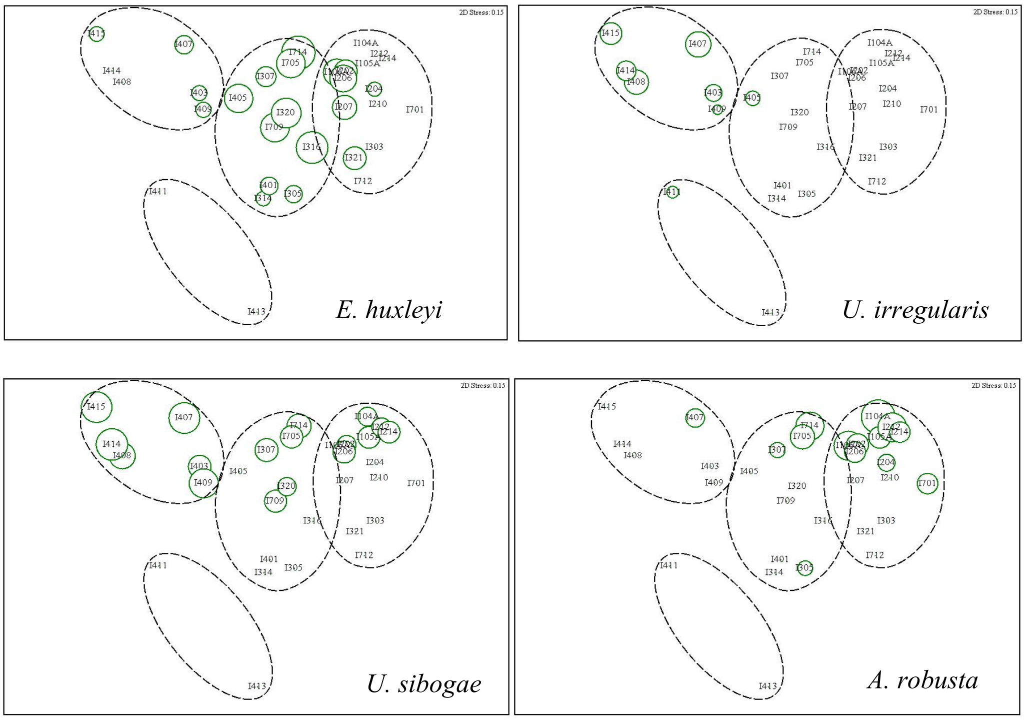

Fig. 14. Stations clustered by Bray-Curtis rank similarities and group average linkage (upper); MDS ordination and its bubble plots for six dominant coccosphere ~~species~~ (below).

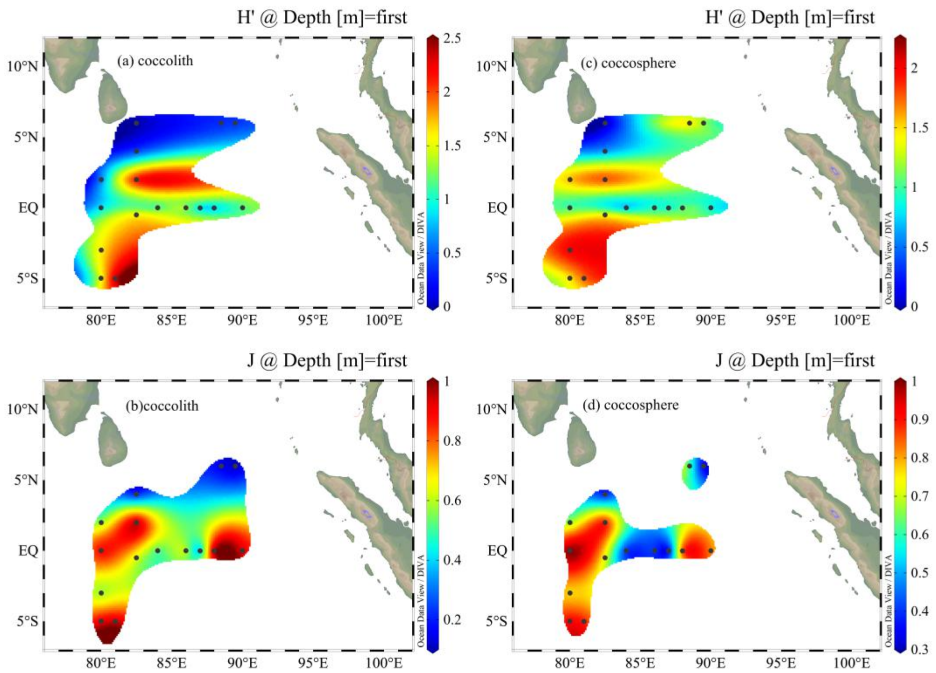

Fig. 15. Surface distributions of biodiversity index of coccolithophore in the surveyed area.

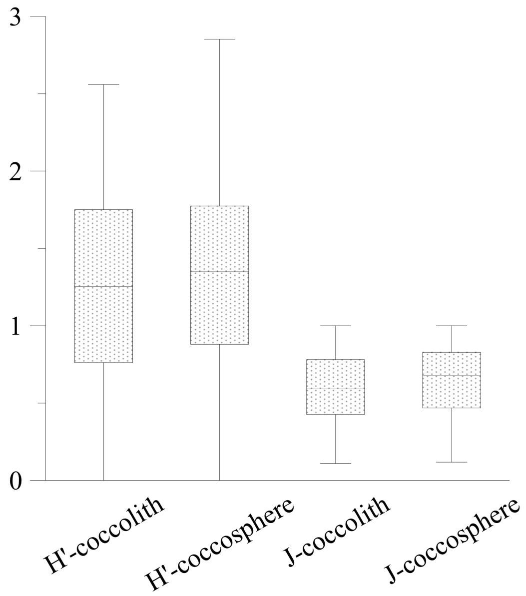

Fig. 16. Box and whisker diagrams of biodiversity index of coccolithophore in the surveyed area.

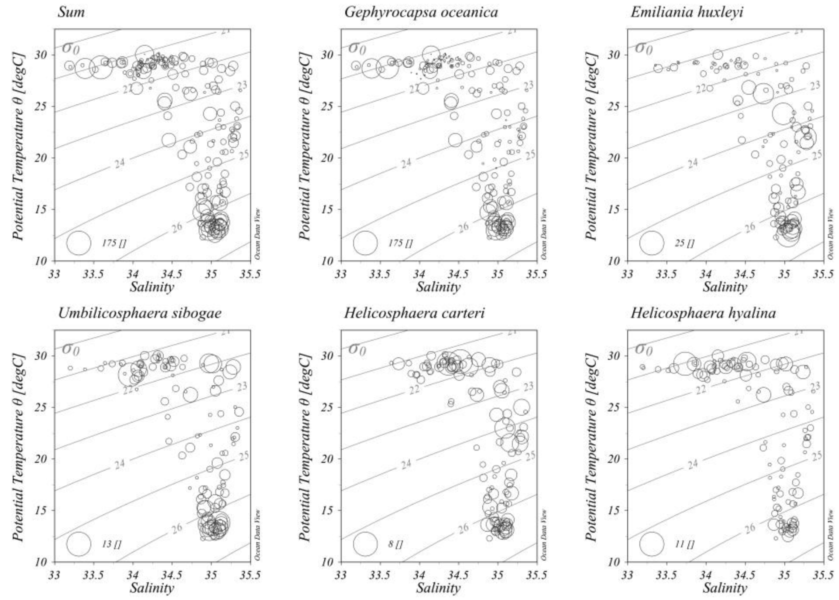

Fig. 17. Scatter plots of coccolith distribution under T-S properties in the surveyed area.

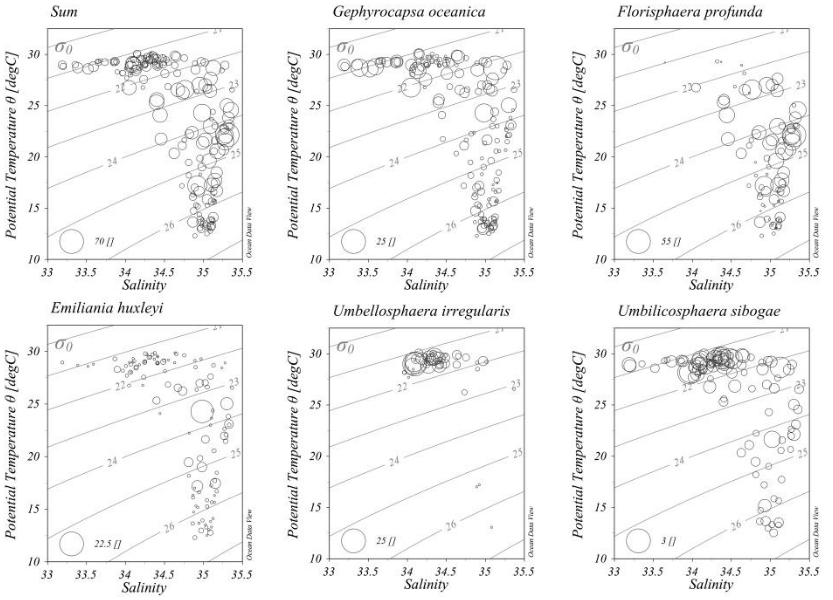

Fig. 18. Scatter plots of coccosphere distribution under T-S properties in the surveyed area.

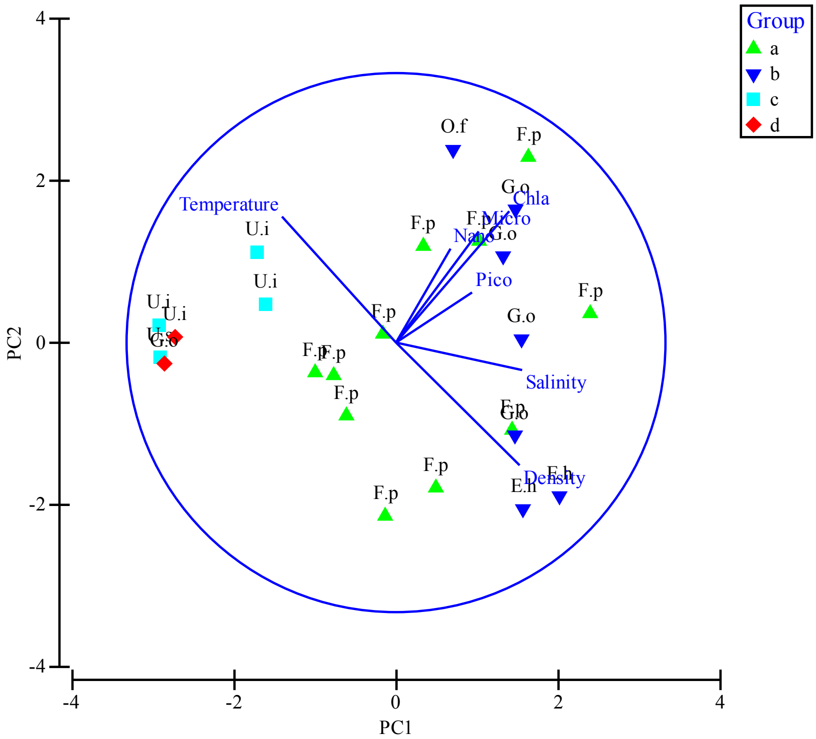

Fig.19. Ordination biplot based on PCA analysis among environmental variables of the surveyed area. Note: group partitions here refer to fig. 13; Chla: chlorophyll, Micro: micro-sized Chla, Nano: nano-sized Chla, Pico: Pico-sized Chla, G.o:*Gephyrocapsa oceanica*, F.p: *Florisphaera profunda*, E.h: *Emiliania huxleyi*, U.i: *Umbellosphaera irregularis*, U.s: *Umbilicosphaera sibogae*, A.r: *Algirosphaera robusta*.

Plate Ⅰ. Noëlaerhabdaceae: *Emiliania*& *Gephyrocapsa*

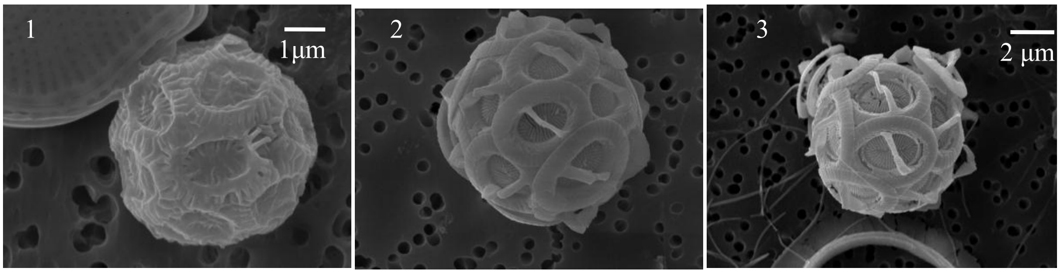

E. huxleyi type A overcalcified*G. oceanica*

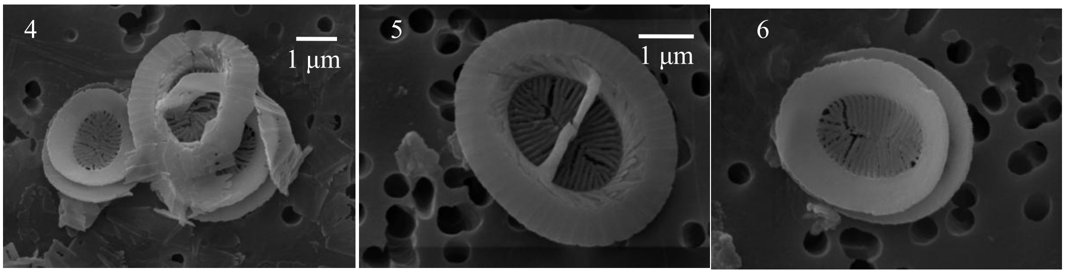

G. oceanica coccolith

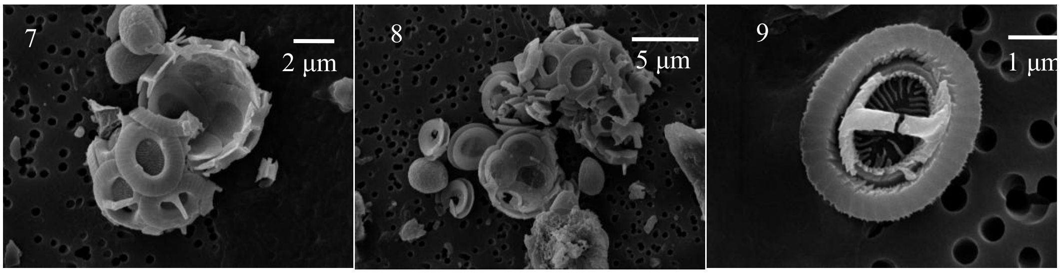

G. oceanica collapsed

Plate Ⅱ. Umbellosphaeraceae: *Umbellosphaera*

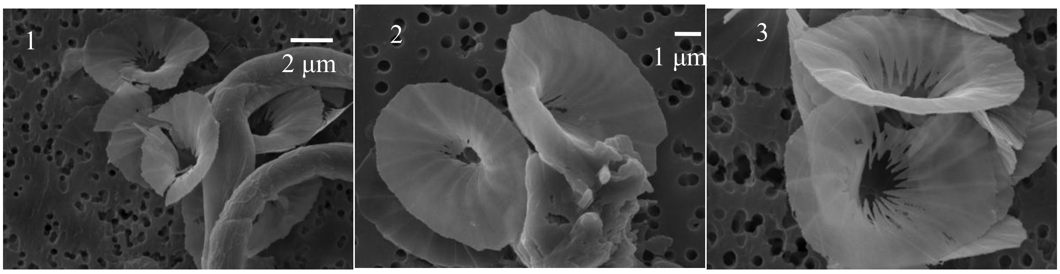

U. irregularis

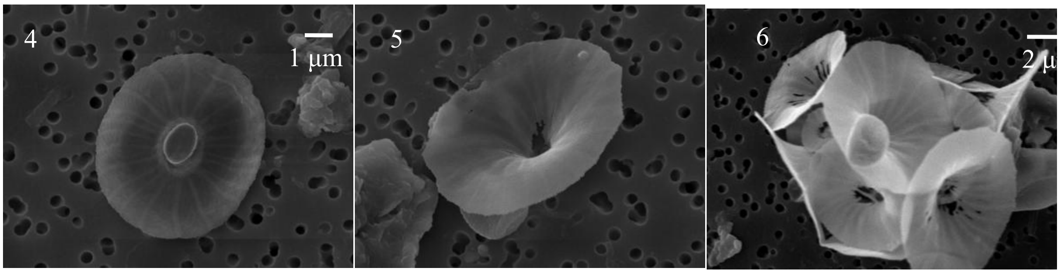

U. irregularis

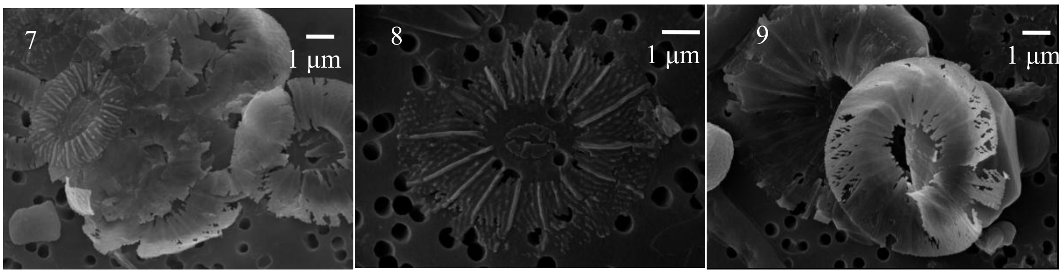

*U. tenuis**U. tenuis* type I

Plate Ⅲ. Calcidiscaceae: *Umbilicosphaera* &*Calcidiscus*

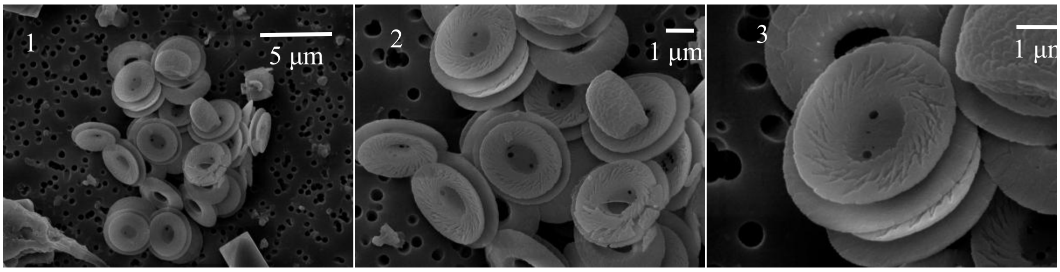

U.hulburtiana

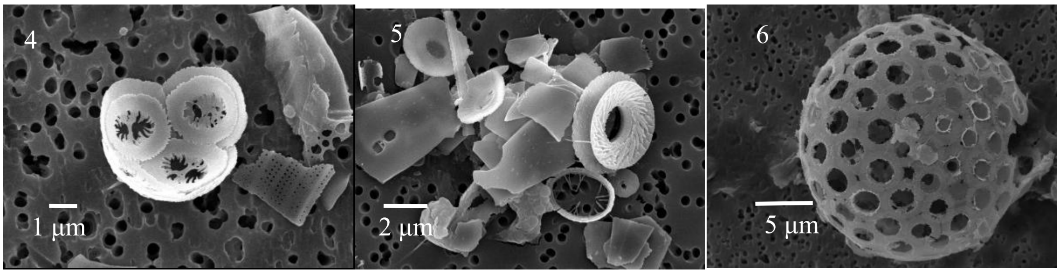

*U. foliosaU. sibogaeU.*sp. 1

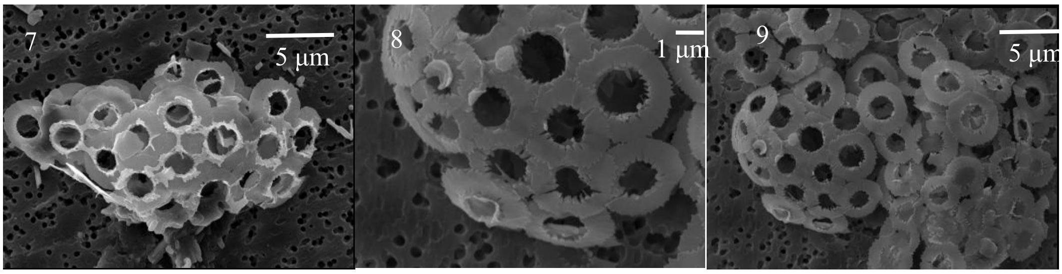

*U.*sp. 1 cell collapsed

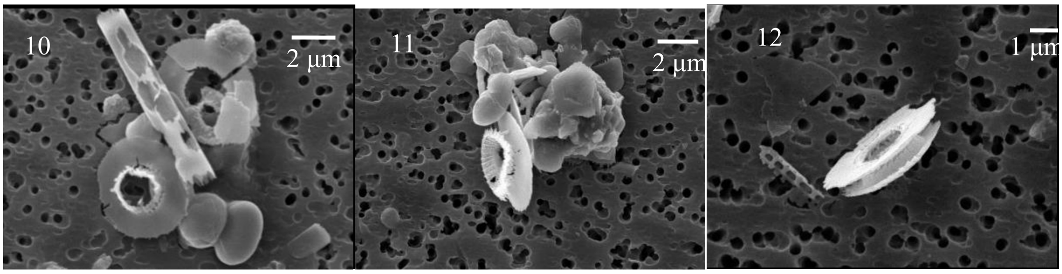

*U.*sp. 1 coccolith detached

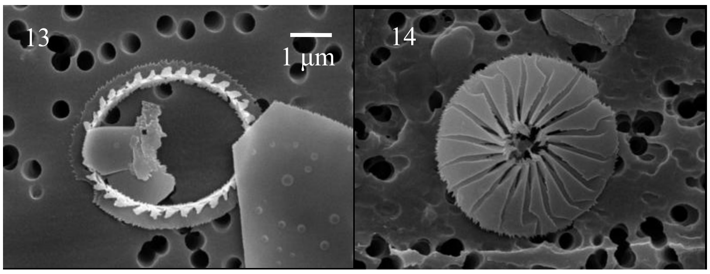

*U.*sp. 2 *C. leptoporus*

Plate Ⅳ.*Reticulofenestra*&*Ceratolithus*&*Pontosphaera*&*Discosphaera*

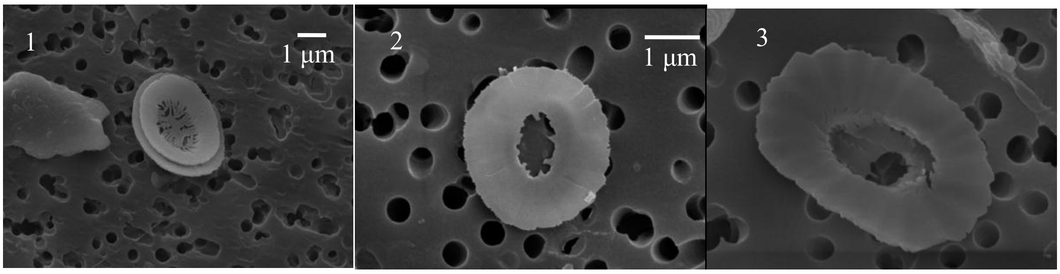

Reticulofenestra sp. 1 *Reticulofenestra* sp. 2

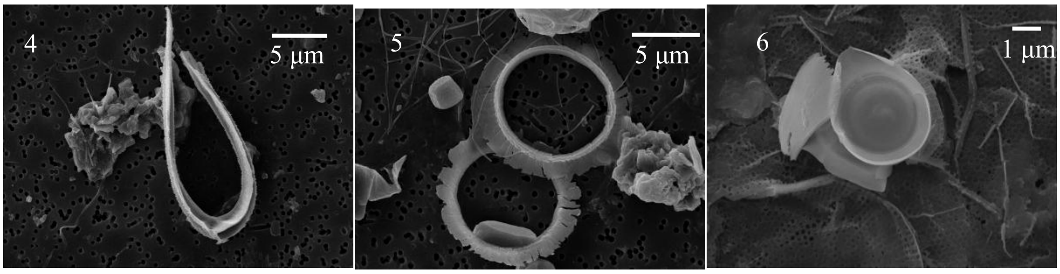

C. cristatus CER *telesmus* type*C. cristatus* HET coccolithomorpha type*P. syracusana*

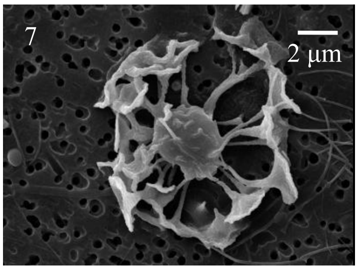

D. tubifera

Plate Ⅴ. Syracosphaeraceae: *Syracosphaera*

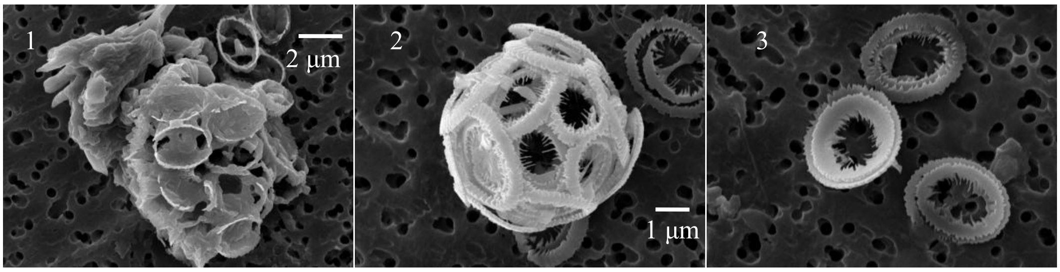

Cell disintegrated*S. histrica*

Plate Ⅵ. Mixed group

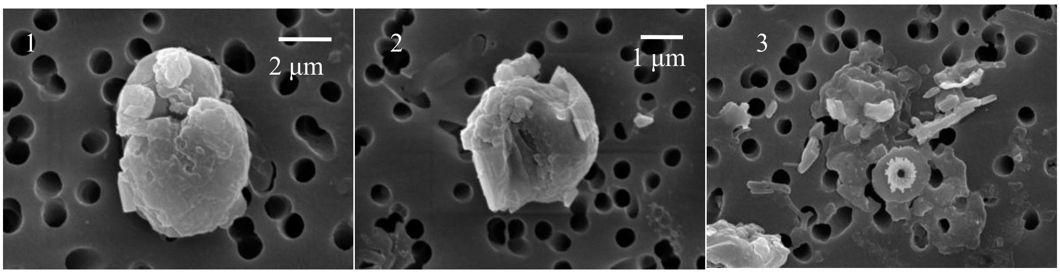

Coccolith-missed coccosphere

Cell collapsed

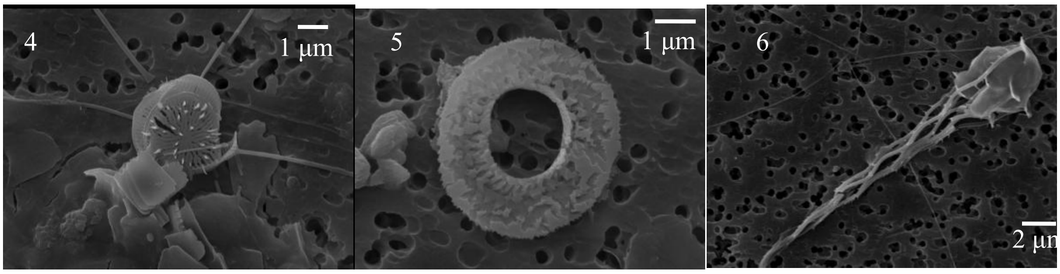

Unknownsp. 1

Unknown sp. 2

Unknown sp. 3

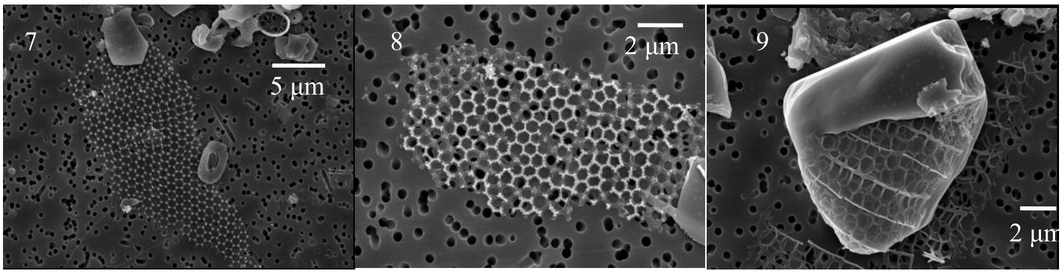

Unknownsp. 3

Unknown sp. 4

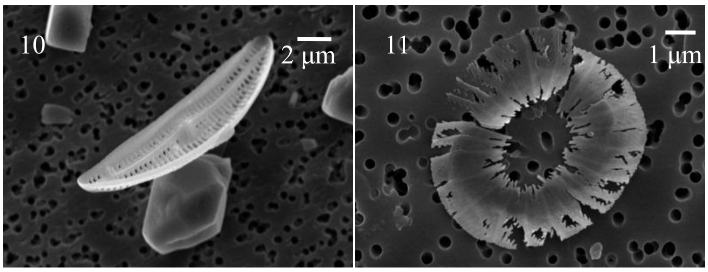

Unknown sp. 4

Coccolith deformed